

# Optimal Regret for Single Index Bandits

Devdan Dey <sup>\*</sup>    Sujoy Bhore <sup>†</sup>    Avishek Ghosh <sup>‡</sup>

## Abstract

We study the *single-index bandit* problem, where rewards depend on an unknown one-dimensional projection of high-dimensional contexts through an unknown reward function. This model extends linear and generalized linear bandits to a nonparametric setting, and is particularly relevant when the reward function is not known in advance. While optimal regret guarantees are known for monotone reward functions, the general non-monotone case remains poorly understood, with the best known bound being  $\tilde{O}(T^{3/4})$  (under standard boundedness and Lipschitz assumptions on the reward function Kang et al. [2025]).

We close this gap by establishing the optimal regret for general single-index bandits. We propose a simple two-phase algorithm, namely, Zoomed Single Index Bandit with Upper Confidence Bound (ZOOMSIB-UCB), that first estimates the projection direction via a normalized Stein estimator, and then reduces the problem to a one-dimensional bandit using discretization and finally use UCB. This approach achieves a regret of  $\tilde{O}(T^{2/3})$ , and improves significantly upon prior work without any additional assumptions. We also prove a matching minimax lower bound of  $\tilde{\Omega}(T^{2/3})$ , showing that the upper bound is essentially tight. Our upper and lower bounds together provide a sharp characterization of the regret in single-index bandits. Moreover, the empirical results further demonstrate the effectiveness and robustness of our approach.

## 1 Introduction

In a single index model (SIM) on data  $(x, y) \in \mathbb{R}^d \times \mathbb{R}$ , we let  $y$  depend on the projection of  $x$  onto an unknown parameter  $\theta_*$  via an unknown function  $f : \mathbb{R} \rightarrow \mathbb{R}$ . Hence, learning in SIM is nonparametric since we need to estimate the parameter  $\theta_*$  as well as the unknown function  $f$ . As an extension of the Generalized Linear Model, the SIM is a versatile statistical framework that has been applied across longitudinal data analysis, quantile regression, and econometrics, and has more recently attracted substantial attention from the theoretical deep learning community as a tool for evaluating the ability of neural networks to learn low-dimensional representations, in contrast to kernel methods (Plan and Vershynin [2016], Brillinger [1982], Bruna and Hsu [2025]).

Learning with SIM remains an active area of research. Early foundational work by Ichimura [1993] and Härdle et al. [1993] establish semiparametric efficiency bounds and optimal estimation rates for the SIM in the classical low-dimensional regime. Hornik et al. [1989] and McCullagh and Nelder [1989] connect the SIM to neural networks and generalized linear models respectively. In the statistical learning theory literature, Plan and Vershynin [2016] and Goldstein et al. [2018] study SIMs through the lens of empirical process theory and Gaussian width. More recently, the connection between SIMs and gradient descent on two-layer neural networks has attracted significant attention (Barak et al. [2022], Abbe et al. [2022]).

Recently, there has been significant interest in understanding the single index model in the sequential framework. The multi-armed bandit is a canonical framework in modeling online (sequential) learning and is classically used for recommendation, clinical trials, targeted ads and hyperparameter tuning Lattimore and Szepesvári [2020], Bubeck and Cesa-Bianchi [2012]. Traditionally, in order to incorporate contextual information, a variant of multi armed bandit framework, namely contextual linear bandit Chu et al. [2011], Abbasi-yadkori et al. [2011], Dani et al. [2008],

---

<sup>\*</sup>Department of Computer Science and Engineering, Indian Institute of Technology Bombay. Email: [23d0365@iitb.ac.in](mailto:23d0365@iitb.ac.in)

<sup>†</sup>Department of Computer Science and Engineering, Indian Institute of Technology Bombay. Email: [sujoy@cse.iitb.ac.in](mailto:sujoy@cse.iitb.ac.in)

<sup>‡</sup>Department of Computer Science and Engineering, Indian Institute of Technology Bombay. Email: [avishek\\_ghosh@iitb.ac.in](mailto:avishek_ghosh@iitb.ac.in)

Li et al. [2010] is studied where the reward is assumed to be a linear function of the context. However, in many applications like click through rate in recommendation systems the linear model fails to capture the reward. To address this, Filippi et al. [2010], Li et al. [2017], Zhang et al. [2025], Faury et al. [2020], Abeille et al. [2021] study the generalized linear bandit framework where the reward is assumed to depend on the context via a generalized linear model. Formally, the mean reward at time  $t$  is given by  $f(x^T \theta_*)$  where the reward function  $f(\cdot)$  is known in advance.

Although such a model captures a lot of practical application, assumption about the knowledge of  $f(\cdot)$  is often unrealistic and it has been shown in Ghosh et al. [2017], Bogunovic and Krause [2021] that misspecification can lead to linear regret. To address this issue, Kang et al. [2025] introduce single index bandit, where the reward function is not known in advance. When the reward function is monotone, the authors of Kang et al. [2025] show that exploiting the Stein estimator, an optimal regret scaling of  $\mathcal{O}(\sqrt{T})$  is possible where  $T$  is the learning horizon. However, when the reward function is non-monotone, Kang et al. [2025] assumes bounded and Lipschitz structure on the reward function and use kernel based estimator to learn the (unknown) function. Using an explore then commit type algorithm resulting in a regret of  $\tilde{O}(T^{3/4})$ .

There has been a few recent works on single index learning in bandits. For example, in Arya et al. [2026], the authors assume that the reward function comes from a Reproducing Kernel Hilbert Space (RKHS) and exploiting the reproducing property as well as representer theorems, the authors show that in some cases  $\mathcal{O}(\sqrt{T})$  is possible. Moreover, in Ma and Cai [2025] reward functions coming from the intersection of smoothness and monotone function class is studied. The paper also proves matching lower bounds for such smooth monotone functions.

Summarizing the above results, we see that for monotone single index bandits, the optimal regret is well understood in literature. However, for general non-monotone functions (with boundedness and Lipschitz structure), apart from the  $\tilde{O}(T^{3/4})$  regret in Kang et al. [2025], no other results are known to the best of our knowledge. This forms the central question of our work:

*What is the optimal regret scaling for general single index bandit?*

In this paper, we answer the above question in affirmative. We keep the assumptions identical to that of Kang et al. [2025] (i.e., the reward function is bounded and Lipschitz) and obtain an improved regret bound of  $\tilde{O}(T^{2/3})$ . We leverage tools from the Lipschitz bandit literature Kleinberg [2004], Kleinberg et al. [2008], Agrawal [1995], Auer et al. [2007], Slivkins [2019] and propose an algorithm that uses discretization and an appropriately instantiated Upper Confidence Bound (UCB) algorithm. Moreover, we prove a minimax lower bound of  $\tilde{\Omega}(T^{2/3})$  implying that no bandit algorithm can incur better regret in the single index setting. Combining these two results, we answer the aforementioned question that the correct regret scaling for general (non-monotone) single index bandit is  $\Theta(T^{2/3})$  (ignoring log factors). We now summarize our contributions.

## 1.1 Summary of contributions

*Improved Regret:* We propose a learning algorithm namely Zoomed Single Index Bandit with Upper Confidence Bound (ZoomSIB-UCB) in Section 3. On a high level, the algorithm breaks the single index learning to a sequence of one-dimensional bandit problems. In the first phase of ZoomSIB-UCB, we use the Stein estimator Stein [1981] with proper normalization and leverage the Lipschitz property of the reward function to discretize the reward space with appropriate resolution into  $N$  bins. In the second phase, we play UCB over  $N$  bins to choose the arm and observe the associated reward. It turns out that  $N \sim T^{1/3}$  is sufficient and as a result the regret of ZoomSIB-UCB is  $\tilde{O}(T^{2/3})$ . This may be seen as a direct improvement over Kang et al. [2025].

*Matching Lower Bound:* We show that the  $\tilde{O}(T^{2/3})$  regret scaling is unavoidable via a lower bound. Formally, we prove a minimax lower bound showing that there exists a problem instance such that *any* learning algorithm suffers a regret of  $\Omega(T^{2/3})$ . Hence, our proposed algorithm is optimal. We construct a one dimensional problem with *bumps* respecting the Lipschitz property. Even in this simple framework, we perturb the problem instance and using information theoretic framework, show that a regret lower bound of  $\tilde{\Omega}(T^{2/3})$ . This implies that ZoomSIB-UCB is optimal. To the best of our knowledge, this is the first work to obtain a minimax lower bound for general non-monotone reward functions.

*Simulation:* We demonstrate the empirical robustness of ZoomSIB-UCB through extensive simulations on complex synthetic geometries and high-dimensional real-world datasets (Section 6). Our results confirm that our approach strictly supersedes the previous state-of-the-art GSTOR Kang et al. [2025] in all respects, consistently achieving substantially lower cumulative regret across every evaluated environment.

### 1.1.1 Novelty and Technical Challenges

The algorithm with improved regret bound and the matching lower bounds comes with significant technical challenges, which we succinctly summarize here. Our proposed algorithm ZoomSIB-UCB uses the notion of zooming and discretization popular in Lipschitz bandits Slivkins [2019], Kleinberg [2004] along with the framework of sleeping bandits Kanade et al. [2009], Kleinberg et al. [2010]. We first argue that a discretization leading to  $N \sim T^{1/3}$  bins is enough in the first phase. A distinctive feature of ZoomSIB-UCB is that only a random subset of bins is available to the learner. Hence, a standard UCB treating all  $N$  bins as viable options would be incorrect. Sleeping bandit Kleinberg et al. [2010] accounts for this by comparing the current reward to the best available bin (see Algorithm 1 for details). Note that a naive application of zooming based algorithm (which is typical in Lipschitz bandits) does not necessarily provide guarantees for single index model, as we need to estimate the underlying parameter  $\theta_*$  along with learning the function simultaneously. We leverage a normalized Stein estimator, zooming based approach and sleeping bandits concurrently to complete the job.

For the minimax lower bound, construction of a hard problem instance and its perturbation is quite non-trivial. We consider a reward function by embedding small plateaued bump of height  $\sim T^{-1/3}$ . This generates a family of  $2^{T^{1/3}}$  functions that are almost identical except bumps (perturbation). We then reduce this to  $T^{1/3}$  armed bandit problem. Finally we define 2 functions that differ in one bump and show that since the bump is of small height, distinguishing the two functions require huge exploration. Formally, using information theoretic tool like Bretagnolle-Huber inequality, we characterize this exploration, leading to an overall regret of  $\tilde{\Omega}(T^{2/3})$ .

## 1.2 Notation

For integer  $r$ ,  $[r]$  denotes the set  $\{1, \dots, r\}$ . The notation  $\tilde{O}(\cdot)$  and  $\tilde{\Omega}(\cdot)$  hides polylogarithmic terms. We use  $\text{polylog}(m)$  to denote polylogarithmic terms in  $m$  with sufficiently large constant degree.

## 2 Setup and Preliminaries

We consider the sequential decision-making problem formulated as a Single-Index Bandit (SIB) Kang et al. [2025]. Let  $T$  denote the time horizon. At each round  $t \in [T]$ , the learner observes an arm set  $\mathcal{X}_t = \{x_{t,a} \in \mathbb{R}^d : a \in [K]\}$  consisting of  $K$  feature vectors. We assume these context vectors are drawn i.i.d. from a continuous distribution  $\mathcal{D}$  with a multivariate probability density function  $p(\cdot)$ .

The learner selects an arm  $x_t \in \mathcal{X}_t$  and observes a stochastic reward:

$$y_t = f(x_t^\top \theta_*) + \eta_t$$

where  $\theta_* \in \mathbb{R}^d$  is the unknown true parameter vector,  $\eta_t$  is zero-mean noise with a finite variance bounded by  $\sigma^2$ , and  $f : \mathbb{R} \rightarrow \mathbb{R}$  is an unknown, continuously differentiable link function.

*Model Identifiability:* One needs to address two issues regarding identifiability in the single index model- (a) scaling and (b) direction (sign). To ensure scaling, we adopt the standard normalization  $\|\theta_*\|_1 = 1$  (see Kang et al. [2025])<sup>1</sup>. Moreover, a quantity of interest for single index model is  $\mu^* = \mathbb{E}[f'(X^T \theta_*)]$  where  $X \sim \mathcal{D}$ . Similar to Kang et al. [2025] (see Section on general function), we assume  $\mu^* > 0$  to resolve the direction identifiability.

*Cumulative Regret:* Let  $x_{t,*} := \arg \max_{x \in \mathcal{X}_t} x^\top \theta_*$  denote the feature vector of the optimal arm at round  $t$ . The performance of the learner is measured by the cumulative regret over  $T$  rounds, defined as the cumulative difference

<sup>1</sup>Another option is  $\ell_2$  normalization. Our choice of  $\ell_1$  normalization has no resemblance to sparsity. Our proposed algorithm uses a discretization which is more tailored to the  $\ell_1$  norm.

between the expected reward of the optimal arm and the chosen arm:

$$R_T = \sum_{t=1}^T (f(x_{t,*}^\top \theta_*) - f(x_t^\top \theta_*))$$

## 2.1 Stein’s Identity and Parameter Estimation

Because the reward function  $f(\cdot)$  is completely unknown, standard generalized linear bandit (GLB) estimators (such as maximum likelihood) are intractable. To bypass this structural limitation, we leverage Stein’s method [Stein \[1981\]](#).

**Definition 2.1** (Score Function). The score function  $S^p : \mathbb{R}^d \rightarrow \mathbb{R}^d$  associated with the density  $p(x)$  is defined as:  $S^p(x) = -\nabla_x \log(p(x)) = -\frac{\nabla_x p(x)}{p(x)}$ .

For readability, we omit the superscript  $p$  and simply write  $S(x)$  when the underlying distribution is clear from the context.

**Stein’s Identity:** By the Generalized Stein’s Lemma, for any continuously differentiable function  $f$ , it holds that  $\mathbb{E}[f(X)S(X)] = \mathbb{E}[\nabla f(X)]$  [Stein \[1981\]](#). Applying this to our specific reward model yields:

$$\mathbb{E}[y_t S(x_t)] = \mathbb{E}[f(x_t^\top \theta_*) S(x_t)] = \mathbb{E}[f'(x_t^\top \theta_*)] \theta_* := \mu_* \theta_*$$

This identity demonstrates that the expected value of the reward, when weighted by the score function, perfectly aligns with the direction of the true parameter  $\theta_*$  (scaled by a constant  $\mu_*$ ) [Stein \[1981\]](#), [Kang et al. \[2025\]](#). This allows the learner to construct an unbiased estimator for the direction of  $\theta_*$  entirely without requiring the explicit form of  $f(\cdot)$ .

## 2.2 The Truncated Stein Estimator

Given  $n$  independent and identically distributed samples  $\{(x_i, y_i)\}_{i=1}^n$ , the naive empirical approach would be to compute the sample average  $\frac{1}{n} \sum_{i=1}^n y_i S(x_i)$ . However, as shown in [Kang et al. \[2025\]](#), a truncation is typically required to control the tails. Let  $\varphi_\tau : \mathbb{R}^d \rightarrow \mathbb{R}^d$  denote an element-wise truncation function

$$[\varphi_\tau(v)]_j = \text{sgn}(v_j) \min(|v_j|, \tau), \quad \forall j \in [d]$$

where  $\tau > 0$  is a carefully chosen truncation threshold. The unnormalized truncated Stein estimator is then defined as

$$\hat{\theta} = \frac{1}{n} \sum_{i=1}^n \varphi_\tau(y_i S(x_i)) \tag{1}$$

To resolve identifiability, we define the normalized estimator as  $\hat{\theta}_0 = \hat{\theta} / \|\hat{\theta}\|_1$ . We now establish the high-probability error bound for the normalized estimator  $\hat{\theta}_0$ .

**Lemma 2.1** (Normalized Stein Estimation Error). *Suppose the unnormalized truncated Stein estimator satisfies  $\|\hat{\theta} - \mu^* \theta^*\|_1 \leq \epsilon$  with probability at least  $1 - \delta$ , where  $\epsilon = C_\theta d \sqrt{\frac{\log(2d/\delta)}{n}}$ . Assume  $\mu^* > 0$ ,  $\|\theta^*\|_1 = 1$ , and that the sample size  $n$  is sufficiently large such that  $\epsilon \leq \mu^*/2$ . Then, with probability at least  $1 - \delta$ , the normalized estimator satisfies,  $\|\hat{\theta}_0 - \theta^*\|_1 \leq \frac{4\epsilon}{\mu^*}$ .*

Note that unlike [Kang et al. \[2025\]](#) the above gives a guarantee on the estimation of  $\theta^*$ , not a scaled version of it.

**Remark 2.2** (On Normalization and Norm Selection). Lemma 2.1 demonstrates that the  $\ell_1$ -normalization step does not degrade the fundamental convergence rate of the unnormalized estimator.

## 3 Algorithm

We discuss our proposed algorithm Zooming Single Index Bandit with UCB (ZoomSIB-UCB)

### 3.1 Overview

ZoomSIB-UCB operates in two sequential phases. The high-level idea is to reduce the original high-dimensional contextual bandit problem to a sequence of one-dimensional bandit problems by exploiting the single-index structure. Since the reward depends on  $x^\top \theta^*$  alone, if we had access to  $\theta^*$  we could project every arm’s context onto the real line and simply run a standard bandit algorithm on the resulting scalar values. Because  $\theta^*$  is unknown, we must first estimate it, and then carefully account for the estimation error when making decisions.

**Phase 1 (Parameter Estimation).** The algorithm dedicates the first  $T_0$  rounds to estimating the unknown index direction  $\theta^*$ .

*The Procedure:* During this phase, it pulls arms uniformly at random, collecting observations that are fed into the Stein-score estimator. The estimator produces  $\hat{\theta}$  satisfying  $\|\hat{\theta} - \mu^* \theta^*\|_1 \leq \epsilon$  with high probability. We then work with the  $\ell_1$ -normalised version  $\hat{\theta}_0 := \hat{\theta} / \|\hat{\theta}\|_1$ , which estimates  $\theta^*$  directly.

*The Calibration:* The exploration length  $T_0$  is calibrated so that the resulting estimation error satisfies:

$$\|\hat{\theta}_0 - \theta^*\|_1 \leq \frac{\Delta}{2L}, \quad (2)$$

where  $\Delta = T^{-1/3}$  is the bin width chosen for Phase 2 and  $L = 4\sqrt{\log(dT/\delta)}$  is a high-probability upper bound on  $\|x_{t,a}\|_\infty$ .

This precise calibration is what makes the two phases mesh together: it guarantees that using  $\hat{\theta}_0$  in place of  $\theta^*$  displaces each arm’s projected index by at most  $\Delta/2$ , i.e., at most half a bin width.

**Phase 2 (UCB over Bins).** Once  $\hat{\theta}_0$  is computed, the algorithm discretises the real line into  $N = O(T^{1/3})$  bins  $B_1, \dots, B_N$  of width  $\Delta$ , centred symmetrically around zero within the window  $[-W, W]$ , where  $W = 4\sqrt{\log(T/\delta)}$  captures all realistic index values with high probability. At each subsequent round  $t$ , the algorithm:

1. Projects each of the  $K$  presented arms onto the estimated index:  $\hat{z}_{t,a} = x_{t,a}^\top \hat{\theta}_0$ .
2. Determines which bin each arm falls into, forming the available bin set  $\mathcal{B}_t \subseteq [N]$ .
3. Runs UCB over the available bins—selecting the arm whose bin has the highest UCB index—and updates the sufficient statistics (pull count  $n_j$  and reward sum  $S_j$ ) for that bin.

The core modelling assumption for Phase 2 is that all arms assigned to the same bin  $B_j$  have nearly the same mean reward, approximated by  $\mu_j := f(\tilde{z}_j)$  where  $\tilde{z}_j$  is the bin centre. The within-bin approximation error is at most  $L_f \Delta$  by the Lipschitzness of  $f$ , and the estimation-induced displacement from Phase 1 adds a further  $\Delta/2$  shift to the true index. Therefore, the total per-arm model error is bounded by  $L_f \Delta$ . This slack is absorbed into an inflated UCB confidence radius, and the discretisation bias accumulated over  $T$  rounds contributes  $O(L_f T^{2/3})$  to the regret.

*Connection to zooming algorithms:* Standard zooming algorithms for Lipschitz bandits maintain an adaptive cover of the arm space: bins are created and refined on the fly, with finer resolution near high-reward regions. ZoomSIB-UCB instead uses a uniform partition of the projected index line at a fixed resolution  $\Delta = T^{-1/3}$ . The “zooming” here is therefore not adaptive in the classical sense—it is a one-shot reduction from a  $d$ -dimensional arm space to a uniform grid on  $\mathbb{R}$ , made possible by the single-index structure. The choice of  $\Delta = T^{-1/3}$  directly resolves the fundamental bias-variance trade-off for discretizing Lipschitz functions. Grouping continuous arms into bins of width  $\Delta$  introduces a per-round approximation bias of  $O(\Delta)$ , accumulating to  $O(T\Delta)$  regret over the horizon. Conversely, making the bins finer increases the total number of bins  $N \approx 1/\Delta$ . The statistical cost to explore  $N$  arms using UCB is  $O(\sqrt{NT}) = O(\sqrt{T/\Delta})$ . Minimising the total regret  $O(T\Delta + \sqrt{T/\Delta})$  by balancing these two terms yields the optimal width  $\Delta = T^{-1/3}$ . At this resolution, the number of bins is  $N = O(T^{1/3})$ , ensuring both the discretization bias and the exploration regret scale at the optimal  $O(T^{2/3})$  rate.

*Connection to sleeping experts and bandits:* A distinctive and non-trivial feature of the algorithm is that at each round  $t$  only a random subset  $\mathcal{B}_t$  of bins is actually available: a bin  $j$  is present in  $\mathcal{B}_t$  only if at least one of the  $K$  freshly drawn arms happens to fall inside  $B_j$ . Since the arms  $x_{t,a}$  are drawn i.i.d. from a continuous distribution each

---

**Algorithm 1** Zooming Single-Index Bandit with UCB ZoomSIB-UCB

---

- 1: **Input:** Total horizon  $T$ , number of arms  $K$ , failure probability  $\delta$ .
- 2: Set maximum arm norm  $L = 4\sqrt{\log(dT/\delta)}$ , truncation window  $W = 4\sqrt{\log(T/\delta)}$ , bin width  $\Delta = T^{-1/3}$ , and total number of bins  $N = \lceil 2W/\Delta \rceil$ .
- 3: Set exploration horizon  $T_0 = \left\lceil d^2 \cdot T^{2/3} \cdot \text{polylog}\left(\frac{dT}{\delta}\right) \right\rceil$ .

**Phase 1: (Parameter Estimation)**

- 4: **for** round  $t = 1, \dots, T_0$  **do**
- 5:   Pull arm  $a_t$  uniformly at random from  $\{1, \dots, K\}$ .
- 6:   Observe reward  $y_t$ .
- 7: **end for**
- 8: Compute unnormalized truncated Stein estimator  $\hat{\theta}$  using samples  $\{(x_{t,a_t}, y_t)\}_{t=1}^{T_0}$  (Eqn 1).
- 9: Compute normalized index estimator  $\hat{\theta}_0 = \hat{\theta}/\|\hat{\theta}\|_1$ .
- 10: Partition  $[-W, W]$  into  $N$  bins  $B_1, \dots, B_N$  of width  $\Delta$ , with centres  $\tilde{z}_j = -W + (j - 1/2)\Delta$ .
- 11: Initialize pull counters  $n_j = 0$  and reward sums  $S_j = 0$  for all bins  $j \in \{1, \dots, N\}$ .

**Phase 2: (UCB over Bins)**

- 12: **for** round  $t = T_0 + 1, \dots, T$  **do**
- 13:   Observe current contexts  $x_{t,a}$  for all  $a \in \{1, \dots, K\}$ .
- 14:   **for** each arm  $a \in \{1, \dots, K\}$  **do**
- 15:     Compute projected context  $\hat{z}_{t,a} = x_{t,a}^\top \hat{\theta}_0$ .
- 16:     Determine the bin assignment index:
$$b_{t,a} = \begin{cases} \lceil (\hat{z}_{t,a} + W)/\Delta \rceil & \text{if } |\hat{z}_{t,a}| \leq W \\ \perp & \text{otherwise} \end{cases}$$
- 17:   **end for**
- 18:   Identify the set of currently available bins  $\mathcal{B}_t = \{b_{t,a} : a \in \{1, \dots, K\}, b_{t,a} \neq \perp\}$ .
- 19:   **if**  $\mathcal{B}_t = \emptyset$  **then**
- 20:     Pull arm  $a_t$  uniformly at random from  $\{1, \dots, K\}$ .
- 21:   **else**
- 22:     **for** each available bin  $j \in \mathcal{B}_t$  **do**
- 23:       Compute the Upper Confidence Bound (UCB) index:

$$\text{UCB}_j(t) = \begin{cases} +\infty & \text{if } n_j = 0 \\ \frac{S_j}{n_j} + \sqrt{\frac{2(\sigma^2 + L_f^2) \log(4NT/\delta)}{n_j}} & \text{if } n_j \geq 1 \end{cases}$$

- 24:     **end for**
  - 25:     Pull arm  $a_t = \arg \max_{\{a: b_{t,a} \in \mathcal{B}_t\}} \text{UCB}_{b_{t,a}}(t)$ .
  - 26:     Observe reward  $y_t$ .
  - 27:     Update bin statistics:  $n_{b_{t,a_t}} = n_{b_{t,a_t}} + 1$  and  $S_{b_{t,a_t}} = S_{b_{t,a_t}} + y_t$ .
  - 28:   **end if**
  - 29: **end for**
- 

round,  $\mathcal{B}_t$  is random and changes with  $t$ . This is precisely the stochastic availability model of sleeping bandits [Kanade et al. \[2009\]](#), [Kleinberg et al. \[2010\]](#). A standard UCB analysis that treats all  $N$  bins as perpetually available would be incorrect as a bin might go many rounds without any arm landing in it, and the UCB indices for absent bins should simply not be considered. The sleeping-UCB analysis correctly accounts for this by comparing the algorithm's reward only to the best available bin  $j_t^* = \arg \max_{j \in \mathcal{B}_t} \mu_j$  at each round, rather than to the globally best bin.

## 4 Regret Analysis

We bound the cumulative regret over the horizon  $T$ . Since the reward function  $f$  is not assumed to be monotonically increasing, the arm with the largest projection does not necessarily yield the highest reward. Let  $a_t^* = \arg \max_{a \in [K]} f(x_{t,a}^\top \theta^*)$  denote the optimal arm at round  $t$ , and define its true index value as  $z_t^* = x_{t,a_t^*}^\top \theta^*$ . The cumulative pseudo-regret is defined as:  $R_T = \sum_{t=1}^T [f(z_t^*) - f(z_{t,a_t})]$ . Here that, we list the assumptions.

### 4.1 Assumptions

**Assumption 1** (Score Moment). There exists a constant  $M > 0$  such that  $\mathbb{E}[S_j(X)^2] \leq M$  for all  $j \in [d]$ , where  $X \sim \mathcal{D}$ .

**Remark 4.1.** This assumption is notably mild. It holds for a wide variety of distributions, including many non-sub-Gaussian and non-zero-mean distributions. It is strictly less restrictive than the finite fourth-moment conditions typically required in the robust estimation literature [Kang et al. \[2025\]](#), [Ma and Cai \[2025\]](#).

**Assumption 2** (Boundedness and Lipschitz Continuity). There exists  $L > 0$  such that  $\|x_{t,i}\|_\infty \leq L$  for all  $i \in [d]$  and  $t \in [T]$ . Furthermore, the unknown reward function and its derivative are uniformly bounded:  $|f(z)| \leq L_f$  and  $|f'(z)| \leq L_{f'}$  for all  $|z| \leq L$ .

**Remark 4.2.** This is a standard condition universally adopted in contextual bandit literature to ensure bounded rewards and controlled variation [Abbasi-yadkori et al. \[2011\]](#), [Dani et al. \[2008\]](#), [Chu et al. \[2011\]](#). The formulation easily accommodates bounding  $L$  at a constant scale up to logarithmic factors (i.e.,  $L = \tilde{O}(1)$ ), which allows the context distribution  $\mathcal{D}$  to be any sub-Gaussian or sub-Exponential distribution [Kang et al. \[2025\]](#).

**Theorem 4.3** (Main Regret Bound). *Suppose Assumptions 1 and 2 hold and that  $\mu^* \geq \frac{c_0}{\text{polylog}(dT/\delta)}$  where  $\delta \in (0, 1)$ ,  $c_0$  is a sufficiently small positive constant. Then, with probability at least  $1 - \delta$ ,*

$$R_T \leq \mathcal{O} \left( d^2 T^{2/3} \text{polylog} \left( \frac{dT}{\delta} \right) \right) = \tilde{O}(d^2 T^{2/3}).$$

Let us discuss the consequences of the above result.

**Remark 4.4** (Improved Regret over [Kang et al. \[2025\]](#)). Note that our result is a direct improvement over [Kang et al. \[2025\]](#), where the authors prove that for general (non-monotone) functions the regret is  $\tilde{O}(T^{3/4})$ . On the other hand, we get an improved regret.

**Remark 4.5** (Dependence on  $d$ ). We obtain a worse dependence on  $d$  compared to [Kang et al. \[2025\]](#). However, this gets amortized by improved dependence on  $T$  as seen in experiments (see [Figure 4](#), [Table 2](#)) even for moderately large  $T$ .

**Condition on  $\mu^*$  and choice of  $T_0$ :** This is a mild quantitative strengthening of the condition  $\mu^* > 0$ . It rules out link functions whose  $\mu^*$  is arbitrarily close to 0. Note that if  $\mu^*$  is very small, then the stein estimator gives (nearly) vacuous results and such an assumption makes it well-behaved. Note that our algorithm does not require the knowledge of  $\mu^*$ . Moreover, in experiments ([Section 6](#)) we use an ‘‘adaptive stopping’’ rule for exploration time  $T_0$  which completely removes the issue of choosing  $T_0$  in practice.

Notably, in [Kang et al. \[2025\]](#) ([Section 3.5](#) for non-monotone functions), the authors implicitly assume the knowledge of  $\mu^*$ , to choose exploration duration for their kernel based estimator and absorb it in the  $\mathcal{O}(\cdot)$  notation making their algorithm non-implementable without knowing  $\mu^*$ . On the other hand, we do not require the knowledge of  $\mu^*$ . As long as it is bounded away from 0, our proposed algorithm works. If we assume the knowledge of  $\mu^*$  similar to [Kang et al. \[2025\]](#), we can remove the condition on  $\mu^*$  as stated in [Theorem 4.3](#) completely. However we believe that the knowledge of  $\mu^*$  is a rather strong assumption, and hence make an attempt to remove it.

## 4.2 Proof Sketch

We first define a good event  $\mathcal{E}$ . On  $\mathcal{E}$ , we show that the estimated and true projected indices are uniformly close:

$$|\hat{z}_{t,a} - z_{t,a}| = |x_{t,a}^\top (\hat{\theta}_0 - \theta^*)| \leq \|x_{t,a}\|_\infty \|\hat{\theta}_0 - \theta^*\|_1 \leq L \left( \frac{\Delta}{2L} \right) = \frac{\Delta}{2} \quad (3)$$

Assuming  $T$  is sufficiently large such that  $\Delta \leq W$ , on  $\mathcal{E}$  every true index satisfies  $|z_{t,a}| \leq W/2$ . Combining this with (3) yields  $|\hat{z}_{t,a}| \leq W/2 + \Delta/2 \leq W$ . This means every arm is successfully assigned to some bin. In particular,  $\mathcal{B}_t \neq \emptyset$  for every  $t > T_0$ , ensuring the algorithm never falls back to the random-pull branch during Phase 2.

Conditioned on  $\mathcal{E}$ , the regret is cleanly decomposed  $R_T = R_T^{(1)} + R_T^{(2)}$  into Phase 1 and Phase 2. Lemma C.1 trivially bounds the uniform exploration cost of Phase 1. For Phase 2, we decompose the instantaneous regret into two parts: (a) discretization bias and (b) (core) bandit regret.

The discretization bias is handled by the Lipschitzness of  $f$  (Lemma C.2). In particular, this yields a regret of  $\mathcal{O}(L_f T^{2/3})$ . The core bandit regret is handled by a novel sleeping-UCB analysis over the stochastic active bin sets (Lemma C.3). For  $N$  bins, the regret scales with  $\sqrt{NT}$ . We choose  $N = \mathcal{O}(T^{1/3})$  (ignoring log factor), which gives the regret from this stage as  $\tilde{\mathcal{O}}(T^{2/3})$ . Finally, combining these two gives the desired bound.

## 5 Minimax Lower Bound

We establish the matching information-theoretic lower bound, demonstrating that no algorithm can achieve a regret scaling of  $\Omega(T^{2/3})$  in the worst case for the general single-index bandit.

**Theorem 5.1** (Minimax Lower Bound). *Let the time horizon  $T$  be sufficiently large. Under the standard regularity conditions (Assumptions 1,2), there exist an absolute constant  $c > 0$  and  $T_0 \in \mathbb{N}$  such that for all  $T \geq T_0$  and every policy  $\pi$ ,*

$$\sup_{(\theta^*, f, \mathcal{D})} \mathbb{E} [R_T(\pi)] \geq cT^{2/3},$$

where the supremum is taken over valid problem instances with ambient dimension  $d = 1$ , parameter  $\theta^* = +1$ , context distribution  $\mathcal{D} = \text{Unif}[-1, 1]$ , and the number of features  $K = \lceil 4T^{1/3} \log T \rceil$ .

**Remark 5.2.** Combined with the  $\tilde{\mathcal{O}}(T^{2/3})$  upper bound established in Theorem 4.3, this confirms that the minimax regret for the non-monotone Single-Index Bandit is strictly  $\Theta(T^{2/3})$ .

### 5.1 Proof Sketch

The lower bound relies on a three-step reduction strategy: construct a family of nearly-identical problem instances, show that any algorithm must be confused between them for a long time, and conclude via information theory that this confusion forces  $\Omega(T^{2/3})$  regret on at least one instance.

**Step 1: Constructing a Localized Hard Family (Section D.1).** We partition the domain  $[-1, 1]$  into  $N = \lceil T^{1/3} \rceil$  equally spaced bins. For each Boolean vector  $\beta \in \{-1, +1\}^N$ , we define a link function  $f_\beta(z)$  by embedding small, plateaued bump functions of height  $\varepsilon = 1/(2N)$  within each bin (Lemma D.1). This generates a family of  $2^N$  functions that are globally identical except for  $\pm\varepsilon$  perturbations localized inside the bins, strictly satisfying the boundedness and Lipschitz assumptions.

**Step 2: Reducing SIB to  $N$ -armed bandit problem (Section D.2).** The primary technical hurdle in the single-index bandit is the “sleeping” structure: at each round, only a random subset of bins contains arms. We remove this complication away by providing a massive menu of arms ( $K = \lceil 4N \log T \rceil$ ) so that, with high probability, every single localized inner bin contains at least one available arm at every round (Lemma D.2). Conditioned on this universal availability event  $\mathcal{E}$ , the sleeping structure vanishes, and the problem collapses into a pure, perpetually available  $N$ -armed stochastic bandit with sub-optimality gaps of  $2\varepsilon$  (Lemma D.3).

**Step 3: The Information-Theoretic Trap (Section D.3).** To trap the algorithm, we isolate a “null” reference hypothesis  $\beta^{(0)}$  (where every bump points downward, making every bin slightly sub-optimal) and  $N$  parallel “spike” hypotheses  $\beta^{(j)}$  (identical to the null, except bin  $j$  is flipped to point upward, making it uniquely optimal). Because the bump height  $\varepsilon$  is extremely small, distinguishing the null from a spike requires massive exploration (Proposition D.1).

The Bretagnolle-Huber inequality formalizes this into an inescapable dilemma for any algorithm: if the algorithm plays conservatively and explores bin  $j$  rarely, it cannot identify the optimal arm when placed in the spike hypothesis; conversely, if it explores aggressively to check for a spike, it suffers heavy regret pulling a downward-pointing bump if the true environment is the null hypothesis. Balancing this bias-variance tradeoff strictly dictates the choice  $N = \Theta(T^{1/3})$ , forcing a minimum expected regret of  $\Omega(T^{2/3})$ .

## 6 Experiments

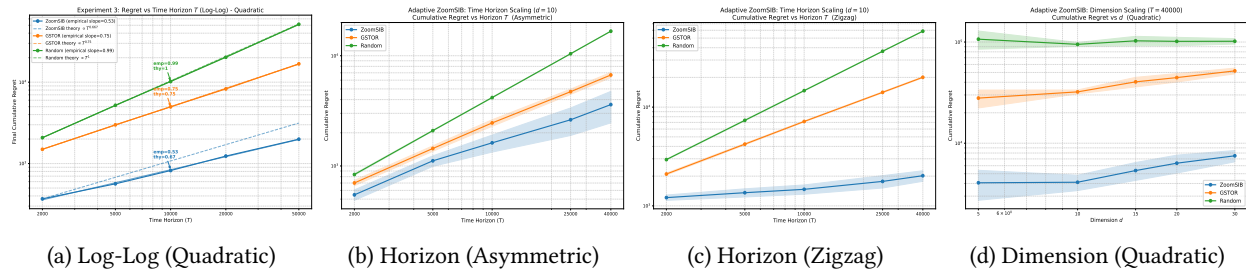


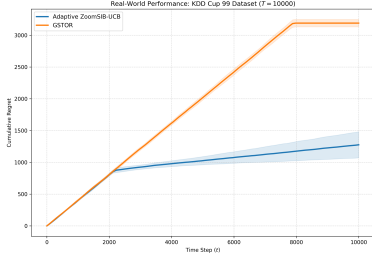
Figure 1: **Comprehensive Synthetic Evaluation.** (a) Log-log regression of cumulative regret. The empirical slope of 0.53 falls strictly below the dashed theoretical limit, confirming robust sublinear scaling. (b, c) Cumulative regret over varying time horizons. ZoomSIB-UCB leverages its early adaptive stopping rule to immediately pull ahead of the GSTOR baseline. (d) Dimension scaling at  $T = 40,000$ . By operating entirely in the projected 1D index space after the initial estimation phase, ZoomSIB-UCB remains highly resilient to massive increases in feature dimension (d).

We evaluate ZoomSIB-UCB against three baselines: GSTOR (non-monotone, kernel-based), ESTOR (monotone-assumed), and Random (uniform selection). We stress-test shape-agnosticism using three synthetic link functions: Quadratic  $f(z) = -(z - 1)^2 + 1$ , Asymmetric  $f(z) = ze^{-z^2}$ , and Zigzag  $f(z) = \sin(z) + 0.3z$ . Default settings:  $d = 10$ , standard Gaussian contexts,  $K = 20$ , averaged over 30 trials ( $\pm 1$  std. dev.).

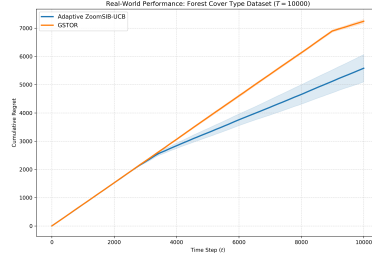
**Adaptive Stopping: No Knowledge of  $T_0$  (or  $\mu^*$ ) Required.** Although theory prescribes  $T_0 = \tilde{O}(d^2 T^{2/3})$ , which can be prohibitively large, we equip ZoomSIB-UCB with an adaptive stopping rule that monitors parameter-estimate stability in real time, autonomously transitioning to exploitation once estimates converge. As shown in Table 1, this self-tuning mechanism exits exploration at just 1.8% of the horizon for easy functions with strong gradients (e.g., Quadratic), while waiting longer for flatter geometries (e.g., Asymmetric).

**Scaling and Theoretical Verification.** ZoomSIB-UCB achieves strictly sublinear regret across all horizons and dimensions, consistently outperforming both baselines (Figure 1b–d). The gap is most pronounced on Quadratic and Zigzag functions, where GSTOR incurs up to 10 $\times$  higher regret at  $T = 40,000$  (Table 1). By compressing  $d$ -dimensional features into a 1D index before arm selection, ZoomSIB-UCB sidesteps the curse of dimensionality: a 6 $\times$  increase in ambient dimension inflates regret by only 2.3 $\times$  (Table 2, Figure 1d).

To verify asymptotic guarantees, we plot regret on a log-log scale (Figure 1a), where slope encodes the scaling exponent. ZoomSIB-UCB achieves an empirical slope of 0.53, well below the theoretical ceiling of  $2/3$  ( $\approx 0.667$ ), confirming optimal scaling and that the worst-case bound is tight only under adversarial conditions. See also Figures 6, 7.



(a) KDD Cup 99 ( $d = 39$ )



(b) Forest Cover Type ( $d = 55$ )

Figure 2: **Real-World Datasets.** Cumulative regret on datasets converted to multi-armed bandit tasks ( $T = 10,000$ ,  $K = 32$ ). Adaptive ZoomSIB-UCB successfully detects early signal convergence, bypassing the catastrophic 79%-89% exploration phases forced upon GSTOR.

**Real-World Data.** We evaluated ZoomSIB-UCB on two offline classification datasets—KDD Cup 99 and Forest Cover Type—cast as contextual bandit tasks (Figure 2). GSTOR’s rigid constraints force exploration over up to 89% of the horizon, whereas ZoomSIB-UCB’s adaptive mechanism identifies feature patterns early, limiting exploration to just 21%–29% and substantially reducing cumulative regret.

Full experimental setups, tabular data, and misspecification evaluations (where ESTOR catastrophically collapses to linear regret) are detailed in Appendix E.

## 7 Conclusion and Open Problems

This paper resolves an open problem by establishing  $\tilde{\Theta}(T^{2/3})$  as the minimax-optimal regret rate for the non-monotone single-index bandit, improving upon  $\tilde{O}(T^{3/4})$  with the first matching information-theoretic lower bound in this setting. We end the paper with a few open problems. Our analysis relies on the Stein estimator and requires  $\mu^* \neq 0$ ; can an alternative technique be developed? It would also be interesting to explore single-index bandits beyond bounded Lipschitz structure, and to understand the implications of our result in the multi-index setting. We keep these as our future endeavors.

## References

- Yasin Abbasi-yadkori, Dávid Pál, and Csaba Szepesvári. Improved algorithms for linear stochastic bandits. In J. Shawe-Taylor, R. Zemel, P. Bartlett, F. Pereira, and K. Weinberger, editors, *Advances in Neural Information Processing Systems*, volume 24. Curran Associates, Inc., 2011. URL [https://proceedings.neurips.cc/paper\\_files/paper/2011/file/e1d5be1c7f2f456670de3d53c7b54f4a-Paper.pdf](https://proceedings.neurips.cc/paper_files/paper/2011/file/e1d5be1c7f2f456670de3d53c7b54f4a-Paper.pdf).
- Emmanuel Abbe, Enric Boix-Adsera, Matthew Brennan, Guy Bresler, and Mingjia Huang. Merged-staircase property: A necessary and nearly sufficient condition for non-linear learning by gradient methods. In *Proceedings of the 35th Annual Conference on Learning Theory (COLT)*, pages 4782–4887, 2022.
- Marc Abeille, Louis Faury, and Clément Calauzènes. Instance-wise minimax-optimal algorithms for logistic bandits. In *Proceedings of the 24th International Conference on Artificial Intelligence and Statistics (AISTATS)*, pages 3691–3699, 2021.
- Jacob Abernethy, Elad Hazan, and Alexander Rakhlin. Competing in the dark: An efficient algorithm for bandit linear optimization. In *Proceedings of the 21st Annual Conference on Learning Theory (COLT)*, pages 263–274, 2008.
- Rajeev Agrawal. Continuum-armed bandit problem. *SIAM Journal on Control and Optimization*, 33(6):1926–1951, 1995.

- Sakshi Arya, Satarupa Bhattacharjee, and Bharath K Sriperumbudur. Kernel single-index bandits: Estimation, inference, and learning. *arXiv preprint arXiv:2603.18938*, 2026.
- Peter Auer. Using confidence bounds for exploitation-exploration trade-offs. *Journal of Machine Learning Research*, 3: 397–422, 2002.
- Peter Auer, Ronald Ortner, and Csaba Szepesvári. Improved rates for the stochastic continuum-armed bandit problem. In *Proceedings of the 20th Annual Conference on Learning Theory (COLT)*, pages 454–468, 2007.
- Boaz Barak, Benjamin Edelman, Surbhi Goel, Sham Kakade, Eran Malach, and Cyril Zhang. Hidden progress in deep learning: SGD learns parities near the computational limit. In *Advances in Neural Information Processing Systems (NeurIPS)*, volume 35, 2022.
- Alberto Bietti, Joan Bruna, Clayton Sanford, and Min Jae Song. Learning single-index models with shallow neural networks. In *Advances in Neural Information Processing Systems (NeurIPS)*, volume 35, 2022.
- Ilija Bogunovic and Andreas Krause. Misspecified gaussian process bandit optimization. *Advances in neural information processing systems*, 34:3004–3015, 2021.
- David R Brillinger. A generalized linear model with Gaussian regressor variables. *A Festschrift for Erich L. Lehmann*, pages 97–114, 1982.
- Joan Bruna and Daniel Hsu. Survey on algorithms for multi-index models. *Statistical Science*, 40(3):378–391, 2025.
- Sébastien Bubeck and Nicolo Cesa-Bianchi. Regret analysis of stochastic and nonstochastic multi-armed bandit problems. *arXiv preprint arXiv:1204.5721*, 2012.
- Sébastien Bubeck, Rémi Munos, Gilles Stoltz, and Csaba Szepesvári.  $\mathcal{X}$ -armed bandits. In *Journal of Machine Learning Research*, volume 12, pages 1655–1695, 2011.
- Sébastien Bubeck, Nicolò Cesa-Bianchi, and Sham M Kakade. Towards minimax policies for online linear optimization with bandit feedback. In *Proceedings of the 25th Annual Conference on Learning Theory (COLT)*, volume 23, pages 41.1–41.14, 2012.
- Alexandra Carpentier and Rémi Munos. Bandit theory meets compressed sensing for high dimensional stochastic linear bandit. In *Proceedings of the 15th International Conference on Artificial Intelligence and Statistics (AISTATS)*, pages 190–198, 2012.
- Wei Chu, Lihong Li, Lev Reyzin, and Robert Schapire. Contextual bandits with linear payoff functions. In Geoffrey Gordon, David Dunson, and Miroslav Dudík, editors, *Proceedings of the Fourteenth International Conference on Artificial Intelligence and Statistics*, volume 15 of *Proceedings of Machine Learning Research*, pages 208–214, Fort Lauderdale, FL, USA, 11–13 Apr 2011. PMLR. URL <https://proceedings.mlr.press/v15/chu11a.html>.
- Alexandru Damian, Jason Lee, and Mahdi Soltanolkotabi. Neural networks can learn representations with gradient descent. In *Conference on Learning Theory*, pages 5413–5452. PMLR, 2022.
- Varsha Dani, Thomas P Hayes, and Sham M Kakade. Stochastic linear optimization under bandit feedback. In *Proceedings of the 21st Annual Conference on Learning Theory (COLT)*, pages 355–366, 2008.
- Miroslav Dudík, Daniel Hsu, Satyen Kale, Nikos Karampatziakis, John Langford, Lev Reyzin, and Tong Zhang. Efficient optimal learning for contextual bandits. In *Proceedings of the 27th Conference on Uncertainty in Artificial Intelligence (UAI)*, pages 169–178, 2011.
- Louis Faury, Marc Abeille, Clément Calauzènes, and Olivier Fercoq. Improved optimistic algorithms for logistic bandits. In *Proceedings of the 37th International Conference on Machine Learning (ICML)*, pages 3052–3062, 2020.

- Sarah Filippi, Olivier Cappé, Aurélien Garivier, and Csaba Szepesvári. Parametric bandits: The generalized linear case. In J. Lafferty, C. Williams, J. Shawe-Taylor, R. Zemel, and A. Culotta, editors, *Advances in Neural Information Processing Systems*, volume 23. Curran Associates, Inc., 2010. URL [https://proceedings.neurips.cc/paper\\_files/paper/2010/file/c2626d850c80ea07e7511bbae4c76f4b-Paper.pdf](https://proceedings.neurips.cc/paper_files/paper/2010/file/c2626d850c80ea07e7511bbae4c76f4b-Paper.pdf).
- Dylan J Foster and Alexander Rakhlin. Beyond ucb: Optimal and efficient contextual bandits with regression oracles. In *Proceedings of the 37th International Conference on Machine Learning (ICML)*, pages 3199–3210, 2020.
- Avishek Ghosh, Sayak Ray Chowdhury, and Aditya Gopalan. Misspecified linear bandits. In *Proceedings of the AAAI Conference on Artificial Intelligence*, volume 31, 2017.
- Larry Goldstein, Ivan Nourdin, and Giovanni Peccati. Structured signal recovery from non-linear and heavy-tailed measurements. *IEEE Transactions on Information Theory*, 64(8):5513–5530, 2018.
- Wolfgang Härdle, Peter Hall, and Hidehiko Ichimura. Optimal smoothing in single-index models. *The Annals of Statistics*, 21(1):157–178, 1993.
- Kurt Hornik, Maxwell Stinchcombe, and Halbert White. Multilayer feedforward networks are universal approximators. *Neural Networks*, 2(5):359–366, 1989.
- Hidehiko Ichimura. Semiparametric least squares (SLS) and weighted SLS estimation of single-index models. *Journal of Econometrics*, 58(1-2):71–120, 1993.
- Kwang-Sung Jun, Rebecca Willett, Stephen Wright, and Robert Nowak. Bilinear bandits with low-rank structure. In *Proceedings of the 36th International Conference on Machine Learning (ICML)*, pages 3163–3172, 2019.
- Sham M Kakade, Adam Tauman Kalai, Varun Kanade, and Ohad Shamir. Efficient learning of generalized linear and single index models with isotonic regression. In *Advances in Neural Information Processing Systems (NeurIPS)*, volume 24, pages 927–935, 2011.
- Adam Tauman Kalai and Ramprasad Sastry. The isotron algorithm: High-dimensional isotonic regression. In *Proceedings of the 22nd Annual Conference on Learning Theory (COLT)*, 2009.
- Varun Kanade, H. Brendan McMahan, and Brent Bryan. Sleeping experts and bandits with stochastic action availability and adversarial rewards. In David van Dyk and Max Welling, editors, *Proceedings of the Twelfth International Conference on Artificial Intelligence and Statistics*, volume 5 of *Proceedings of Machine Learning Research*, pages 272–279, Hilton Clearwater Beach Resort, Clearwater Beach, Florida USA, 16–18 Apr 2009. PMLR. URL <https://proceedings.mlr.press/v5/kanade09a.html>.
- Yue Kang, Mingshuo Liu, Bongsoo Yi, Jing Lyu, Zhi Zhang, Doudou Zhou, and Yao Li. Single index bandits: Generalized linear contextual bandits with unknown reward functions. *arXiv preprint arXiv:2506.12751*, 2025.
- Robert Kleinberg, Aleksandrs Slivkins, and Eli Upfal. Multi-armed bandits in metric spaces. In *Proceedings of the 40th Annual ACM Symposium on Theory of Computing (STOC)*, pages 681–690, 2008.
- Robert Kleinberg, Alexandru Niculescu-Mizil, and Yogeshwer Sharma. Regret bounds for sleeping experts and bandits. *Machine learning*, 80(2):245–272, 2010.
- Robert D Kleinberg. Nearly tight bounds for the continuum-armed bandit problem. In *Advances in Neural Information Processing Systems (NeurIPS)*, volume 17, pages 697–704, 2004.
- John Langford and Tong Zhang. The epoch-greedy algorithm for multi-armed bandits with side information. In *Advances in Neural Information Processing Systems (NeurIPS)*, volume 20, pages 817–824, 2008.
- Tor Lattimore and Csaba Szepesvári. *Bandit Algorithms*. Cambridge University Press, 2020.

- Tor Lattimore, Csaba Szepesvári, and Gellért Weisz. Learning with good feature representations in bandits and in rl with a generative model. In *Proceedings of the 37th International Conference on Machine Learning (ICML)*, pages 5662–5670, 2020.
- Lihong Li, Wei Chu, John Langford, and Robert E Schapire. A contextual-bandit approach to personalized news article recommendation. In *Proceedings of the 19th International Conference on World Wide Web (WWW)*, pages 661–670, 2010.
- Lihong Li, Yu Lu, and Dengyong Zhou. Provably optimal algorithms for generalized linear contextual bandits. In *International Conference on Machine Learning*, pages 2071–2080. PMLR, 2017.
- Andrea Locatelli and Alexandra Carpentier. Adaptivity to smoothness in  $x$ -armed bandits. In *Proceedings of the 31st Annual Conference on Learning Theory (COLT)*, pages 1463–1492, 2018.
- Wanteng Ma and T Tony Cai. Nonparametric bandits with single-index rewards: Optimality and adaptivity. *arXiv preprint arXiv:2512.24669*, 2025.
- Stefan Magureanu, Richard Combes, and Alexandre Proutiere. Lipschitz bandits without the Lipschitz constant. In *Proceedings of the 25th International Conference on Algorithmic Learning Theory (ALT)*, pages 144–158, 2014.
- Peter McCullagh and John A Nelder. *Generalized Linear Models*. Chapman and Hall, London, 2nd edition, 1989.
- Rémi Munos. Optimistic optimization of a deterministic function without the knowledge of its smoothness. In *Advances in Neural Information Processing Systems (NeurIPS)*, volume 24, pages 783–791, 2011.
- Yaniv Plan and Roman Vershynin. The generalized lasso with non-linear observations. *IEEE Transactions on Information Theory*, 62(3):1528–1537, 2016.
- Aleksandrs Slivkins. Contextual bandits with similarity information. In *Journal of Machine Learning Research*, volume 15, pages 2533–2568, 2014.
- Aleksandrs Slivkins. Introduction to multi-armed bandits. *Foundations and Trends® in Machine Learning*, 12(1-2): 1–286, 2019.
- Charles M Stein. Estimation of the mean of a multivariate normal distribution. *The Annals of Statistics*, 9(6):1135–1151, 1981.
- Christos Thrampoulidis, Ehsan Abbasi, and Babak Hassibi. Lasso with non-linear measurements is equivalent to one with linear measurements. *Advances in Neural Information Processing Systems (NeurIPS)*, 28:3420–3428, 2015.
- Michal Valko, Alexandra Carpentier, and Rémi Munos. Stochastic simultaneous optimistic optimization. In *Proceedings of the 30th International Conference on Machine Learning (ICML)*, pages 19–27, 2013.
- Yu-Jie Zhang, Sheng-An Xu, Peng Zhao, and Masashi Sugiyama. Generalized linear bandits: Almost optimal regret with one-pass update. *arXiv preprint arXiv:2507.11847*, 2025.

## A Other Related Work

### A.1 Linear Bandits, Contextual Bandits and Generalized Linear Bandits

Linear bandits extend the finite-armed bandit problem to structured continuous action spaces, with [Auer \[2002\]](#) establishing the foundational optimism-under-uncertainty template and [Dani et al. \[2008\]](#) providing the first  $\tilde{O}(d\sqrt{T})$  regret bound via confidence ellipsoids, later sharpened to a tight  $\tilde{O}(d\sqrt{T})$  by the canonical OFUL algorithm of [Abbasi-yadkori et al. \[2011\]](#) using regularized least-squares estimation. The matching  $\Omega(d\sqrt{T})$  lower bound of [Dani et al. \[2008\]](#) confirms optimality. The adversarial setting is studied by [Abernethy et al. \[2008\]](#) and [Bubeck et al. \[2012\]](#), who establish near-optimal  $\tilde{O}(\sqrt{dT})$  bounds, while subsequent work extended the framework to sparsity [[Carpentier](#)

and Munos, 2012], low-rank structure [Jun et al., 2019], and misspecification [Lattimore et al., 2020]. Contextual bandits condition rewards on an observed context vector, with LinUCB [Li et al., 2010] and its theoretical analysis [Chu et al., 2011] achieving  $\tilde{O}(d\sqrt{T})$  regret in the linear case; the agnostic setting is addressed by Langford and Zhang [2008] via epoch-greedy exploration and by Dudík et al. [2011] via oracle reductions, with Foster and Rakhlin [2020] ultimately achieving the optimal  $\tilde{O}(\sqrt{KT})$  rate through regression oracle reductions.

Generalized linear bandits (GLBs) pass the inner product  $\langle \theta, a \rangle$  through a known link function  $\mu(\cdot)$ , with GLM-UCB Filippi et al. [2010] establishing  $\tilde{O}(d\sqrt{T})$  regret under bounded link functions, Li et al. [2017] improving curvature dependence and Faury et al. [2020] achieving refined bounds for logistic bandits via self-concordance. Also Abeille et al. [2021] derive instance-dependent lower bounds that connect GLBs to the broader theory of structured bandits.

## A.2 Single Index Model

Semiparametric efficiency bounds and optimal estimation rates for the SIM in the classical low-dimensional regime are established by Ichimura [1993] and Härdle et al. [1993]. Hornik et al. [1989] and McCullagh and Nelder [1989] connect the SIM to neural networks and generalized linear models respectively, situating it within a broader modeling landscape. In the high-dimensional setting where  $d \gg n$ , Plan and Vershynin [2016] provides a seminal analysis showing that the index vector  $\theta^*$  can be estimated from one-bit compressed measurements at the rate  $O(s \log d/n)$  under sparsity, leveraging the connection between the SIM and generalized linear measurements. Brillinger [1982] has earlier observed that ordinary least squares recovers  $\theta^*$  up to a scalar in the SIM under Gaussian designs, a phenomenon later formalized and extended by Plan and Vershynin [2016] and Thrampoulidis et al. [2015]. The work of Kalai and Sastry [2009] introduce the Isotron algorithm, the first computationally efficient method to jointly learn  $\theta^*$  and  $f$  with provable guarantees under Gaussian covariates. Kakade et al. [2011] subsequently extend these results via the STAP algorithm, achieving polynomial sample and computational complexity for learning SIMs with monotone link functions.

Through the lens of empirical process theory and Gaussian width, the estimation error of convex programs for SIM recovery was characterized in terms of the geometry of the parameter set by Plan and Vershynin [2016] and Goldstein et al. [2018]. More recently, the connection between SIMs and gradient descent on two-layer neural networks has attracted significant attention: Barak et al. [2022] and Abbe et al. [2022] studied the SIM as a prototypical model for understanding what gradient-based methods can and cannot learn, establishing computational-statistical gaps tied to the information exponent of the link function  $f$ . Bietti et al. [2022] and Damian et al. [2022] further showed that a single gradient step on the population loss suffices to recover the index direction up to a polynomial sample complexity, formalizing the so-called leap exponent as the key quantity governing the difficulty of the learning problem under staircase-structured link functions.

## A.3 Lipschitz Bandits

In Agrawal [1995], the authors establish the feasibility of consistent estimation in the one-dimensional setting, and Kleinberg [2004] derived nearly tight  $\tilde{O}(T^{2/3})$  regret bounds, later tightened and connected to nonparametric regression by Auer et al. [2007]. Kleinberg et al. [2008] extend the framework to general metric spaces via the zooming algorithm, achieving instance-dependent regret scaling with the zooming dimension rather than the ambient dimension, with a matching minimax lower bound of  $\Omega(T^{(d+1)/(d+2)})$  for  $d$ -dimensional spaces confirming the tightness of this dependence. The  $X$ -armed bandit framework of Bubeck et al. [2011] introduce the HOO algorithm, which operates on a hierarchical partition of the action space and achieves regret depending on the near-optimality dimension, providing a unified treatment of Lipschitz and smooth bandits; Munos [2011] subsequently develop the parameter-free SOO and StoSOO algorithms, and Valko et al. [2013] extend this line of work to kernel-based methods exploiting RKHS structure. Slivkins [2014] generalize the framework to contextual bandits via a joint similarity metric over contexts and actions, Magureanu et al. [2014] derive instance-dependent logarithmic regret bounds under a margin condition analogous to Tsybakov’s noise condition, and Locatelli and Carpentier [2018] study adaptive algorithms achieving optimal rates across smoothness classes without knowledge of the Lipschitz constant.

## B Proofs

**Lemma B.1** (Normalized Stein Estimation Error). *Suppose the unnormalized truncated Stein estimator satisfies  $\|\hat{\theta} - \mu^* \theta^*\|_1 \leq \epsilon$  with probability at least  $1 - \delta$ , where  $\epsilon = C_\theta d \sqrt{\frac{\log(2d/\delta)}{n}}$ . Assume  $\mu^* > 0$ ,  $\|\theta^*\|_1 = 1$ , and that the sample size  $n$  is sufficiently large such that  $\epsilon \leq \mu^*/2$ . Then, with probability at least  $1 - \delta$ , the normalized estimator satisfies:*

$$\|\hat{\theta}_0 - \theta^*\|_1 \leq \frac{4\epsilon}{\mu^*} = \mathcal{O}\left(d \sqrt{\frac{\log(d/\delta)}{n}}\right) \quad (4)$$

*Proof.* Condition on the high-probability event where the raw estimator bound, as established by Kang et al. [2025], holds:  $\|\hat{\theta} - \mu^* \theta^*\|_1 \leq \epsilon$ .

First, we bound the magnitude of the normalization denominator  $\|\hat{\theta}\|_1$ . By the reverse triangle inequality, we have:

$$|\|\hat{\theta}\|_1 - \|\mu^* \theta^*\|_1| \leq \|\hat{\theta} - \mu^* \theta^*\|_1 \leq \epsilon \quad (5)$$

Since  $\mu^* > 0$  and  $\|\theta^*\|_1 = 1$ , we know  $\|\mu^* \theta^*\|_1 = \mu^* \|\theta^*\|_1 = \mu^*$ . Substituting this in gives:

$$|\|\hat{\theta}\|_1 - \mu^*| \leq \epsilon \quad (6)$$

This implies that  $\|\hat{\theta}\|_1 \in [\mu^* - \epsilon, \mu^* + \epsilon]$ . By the theorem's assumption that the sample size is large enough to ensure  $\epsilon \leq \mu^*/2$ , it strictly follows that  $\|\hat{\theta}\|_1 \geq \mu^*/2 > 0$ .

Next, we evaluate the  $\ell_1$  distance between the normalized estimator  $\hat{\theta}_0$  and the true parameter  $\theta^*$ :

$$\|\hat{\theta}_0 - \theta^*\|_1 = \left\| \frac{\hat{\theta}}{\|\hat{\theta}\|_1} - \theta^* \right\|_1 = \frac{1}{\|\hat{\theta}\|_1} \|\hat{\theta} - \|\hat{\theta}\|_1 \theta^*\|_1 \quad (7)$$

To leverage our existing bound, we add and subtract  $\mu^* \theta^*$  inside the norm:

$$\|\hat{\theta}_0 - \theta^*\|_1 = \frac{1}{\|\hat{\theta}\|_1} \|(\hat{\theta} - \mu^* \theta^*) + (\mu^* \theta^* - \|\hat{\theta}\|_1 \theta^*)\|_1 \quad (8)$$

Applying the standard triangle inequality yields:

$$\|\hat{\theta}_0 - \theta^*\|_1 \leq \frac{1}{\|\hat{\theta}\|_1} \left( \|\hat{\theta} - \mu^* \theta^*\|_1 + \|(\mu^* - \|\hat{\theta}\|_1) \theta^*\|_1 \right) \quad (9)$$

We can factor out the scalar absolute value from the second term:

$$\|\hat{\theta}_0 - \theta^*\|_1 \leq \frac{1}{\|\hat{\theta}\|_1} \left( \|\hat{\theta} - \mu^* \theta^*\|_1 + |\mu^* - \|\hat{\theta}\|_1| \|\theta^*\|_1 \right) \quad (10)$$

Now, we substitute the bounds we established earlier. We know  $\|\hat{\theta}\|_1 \geq \mu^*/2$ ,  $\|\hat{\theta} - \mu^* \theta^*\|_1 \leq \epsilon$ ,  $|\mu^* - \|\hat{\theta}\|_1| \leq \epsilon$ , and  $\|\theta^*\|_1 = 1$ . Plugging these in gives:

$$\|\hat{\theta}_0 - \theta^*\|_1 \leq \frac{1}{\mu^*/2} (\epsilon + \epsilon \cdot 1) = \frac{2}{\mu^*} (2\epsilon) = \frac{4\epsilon}{\mu^*} \quad (11)$$

Substituting the definition of  $\epsilon$ , we conclude the proof:

$$\|\hat{\theta}_0 - \theta^*\|_1 \leq \frac{4C_\theta}{\mu^*} d \sqrt{\frac{\log(2d/\delta)}{n}} \quad (12)$$

which preserves the desired convergence rate.  $\square$

## C Proof of Theorem 4.3

### C.1 High-Probability Events

Before presenting the lemmas, we collect the probabilistic scaffolding on which the entire analysis rests. To ensure the final theorem holds with probability at least  $1 - \delta$ , we scale the failure probability of each individual event to  $\delta/4$ . Define the following four events:

- $\mathcal{E}_1 := \{\|\hat{\theta}_0 - \theta^*\|_1 \leq \Delta/(2L)\}$ , the event that Phase 1 estimation succeeds. By Lemma 2.1 and the choice of  $T_0$ ,  $\mathbb{P}(\mathcal{E}_1) \geq 1 - \delta/4$ .
- $\mathcal{E}_2 := \{\|x_{t,a}\|_\infty \leq L, \forall t \in [T], a \in [K]\}$  where  $L = 4\sqrt{\log(4dT/\delta)}$ . By a Gaussian tail bound and union bound over  $TK$  arms,  $\mathbb{P}(\mathcal{E}_2) \geq 1 - \delta/4$ .
- $\mathcal{E}_3 := \{|x_{t,a}^\top \theta^*| \leq W/2, \forall t \in [T], a \in [K]\}$  where  $W = 4\sqrt{\log(4dT/\delta)}$ . Since  $x_{t,a}^\top \theta^*$  is Gaussian with variance  $\|\Sigma_X^{1/2} \theta^*\|_2^2 \leq \|\Sigma_X^{1/2} \theta^*\|_1^2 = 1$ , a union bound gives  $\mathbb{P}(\mathcal{E}_3) \geq 1 - \delta/4$ .
- $\mathcal{E}_4 := \{|\bar{y}_j - \mu_j| \leq U_j(n_j) + L_f \Delta, \forall j \in [N], \forall n \in [T]\}$ , the UCB concentration event accounting for within-bin approximation bias. By Hoeffding's inequality and a union bound over  $j \in [N]$  and  $n \leq T$ ,  $\mathbb{P}(\mathcal{E}_4) \geq 1 - \delta/4$ .

Throughout the analysis, we work on the intersection event  $\mathcal{E} := \mathcal{E}_1 \cap \mathcal{E}_2 \cap \mathcal{E}_3 \cap \mathcal{E}_4$ , which satisfies  $\mathbb{P}(\mathcal{E}) \geq 1 - \delta$ .

On  $\mathcal{E}_1 \cap \mathcal{E}_2$ , the estimated and true projected indices are uniformly close:

$$|\hat{z}_{t,a} - z_{t,a}| = |x_{t,a}^\top (\hat{\theta}_0 - \theta^*)| \leq \|x_{t,a}\|_\infty \|\hat{\theta}_0 - \theta^*\|_1 \leq L \left( \frac{\Delta}{2L} \right) = \frac{\Delta}{2} \quad (13)$$

Assuming  $T$  is sufficiently large such that  $\Delta \leq W$ , on  $\mathcal{E}_3$  every true index satisfies  $|z_{t,a}| \leq W/2$ . Combining this with (13) yields  $|\hat{z}_{t,a}| \leq W/2 + \Delta/2 \leq W$ . This means every arm is successfully assigned to some bin. In particular,  $\mathcal{B}_t \neq \emptyset$  for every  $t > T_0$ , ensuring the algorithm never falls back to the random-pull branch during Phase 2.

**Proof Roadmap:** Conditioned on  $\mathcal{E}$ , the regret is cleanly decomposed  $R_T = R_T^{(1)} + R_T^{(2)}$  into Phase 1 and Phase 2. Lemma C.1 trivially bounds the uniform exploration cost of Phase 1. For Phase 2, we decompose the instantaneous regret into a discretisation bias—handled via the Lipschitzness of  $f$  (Lemma C.2)—and the core bandit regret, which we bound using a novel sleeping-UCB analysis over the stochastic active bin sets (Lemma C.3).

### C.2 Phase 1 Regret

**Lemma C.1** (Phase 1 Cost). *The regret incurred during Phase 1 satisfies:*

$$R_T^{(1)} \leq 2L_f T_0 = \mathcal{O}\left(d^2 T^{2/3} \text{polylog}\left(\frac{dT}{\delta}\right)\right)$$

*Proof.* Since  $|f| \leq L_f$ , the maximum instantaneous regret at any round is trivially bounded by  $f(z_t^*) - f(z_{t,a_t}) \leq L_f - (-L_f) = 2L_f$ . The Phase 1 length is:

$$T_0 = \left\lceil \left( \frac{4C_\theta L}{\mu^* \Delta} \right)^2 d^2 \log\left(\frac{8d}{\delta}\right) \right\rceil = \mathcal{O}\left(L^2 d^2 \log\left(\frac{8d}{\delta}\right) T^{2/3} \text{polylog}\left(\frac{dT}{\delta}\right)\right)$$

using  $\Delta = T^{-1/3}$  and  $\mu^* \geq c_0/\text{polylog}(Td/\delta)$ . Substituting  $L^2 = 16 \log(4dT/\delta)$  yields the stated bound.  $\square$

### C.3 Phase 2 Regret Decomposition

For  $t > T_0$ , let  $b_t^* = b_{t,a_t^*}$  denote the bin assigned to the optimal available arm, and  $b_t = b_{t,a_t}$  denote the bin of the arm actually played. We decompose the instantaneous regret as:

$$f(z_t^*) - f(z_{t,a_t}) = \underbrace{[f(z_t^*) - \mu_{b_t^*}]}_{(i)} + \underbrace{[\mu_{b_t^*} - \mu_{b_t}]}_{(ii)} + \underbrace{[\mu_{b_t} - f(z_{t,a_t})]}_{(iii)} \quad (14)$$

where  $\mu_j := f(\tilde{z}_j)$  is the true reward evaluated at the bin centre  $\tilde{z}_j$ . Terms (i) and (iii) represent the discretisation bias (the error from approximating a continuous arm's reward by its bin centre). Term (ii) is the bandit regret (the loss from the UCB policy failing to play the best available bin).

**Lemma C.2** (Discretisation Bias). *On  $\mathcal{E}_1 \cap \mathcal{E}_2 \cap \mathcal{E}_3$ , for every  $t > T_0$  and every arm  $a$  assigned to bin  $b_{t,a} = j$ , we have  $|f(z_{t,a}) - \mu_j| \leq L_{f'}\Delta$ . Consequently:*

$$\sum_{t=T_0+1}^T [(i) + (iii)] \leq 2L_{f'}T\Delta = 2L_{f'}T^{2/3}$$

*Proof.* Let arm  $a$  satisfy  $\hat{z}_{t,a} \in B_j$ . By the definition of the bin,  $|\hat{z}_{t,a} - \tilde{z}_j| \leq \Delta/2$ . From (13), we have  $|z_{t,a} - \hat{z}_{t,a}| \leq \Delta/2$ . By the triangle inequality:

$$|z_{t,a} - \tilde{z}_j| \leq |z_{t,a} - \hat{z}_{t,a}| + |\hat{z}_{t,a} - \tilde{z}_j| \leq \frac{\Delta}{2} + \frac{\Delta}{2} = \Delta$$

Since  $|f'| \leq L_{f'}$ , the link function  $f$  is  $L_{f'}$ -Lipschitz, yielding  $|f(z_{t,a}) - \mu_j| = |f(z_{t,a}) - f(\tilde{z}_j)| \leq L_{f'}\Delta$ . Applying this to  $a = a_t^*$  (with  $j = b_t^*$ ) and  $a = a_t$  (with  $j = b_t$ ), and summing over  $T$  rounds gives the aggregate bound.  $\square$

**Lemma C.3** (Sleeping-UCB Regret). *Consider  $N$  bins with means  $\mu_1, \dots, \mu_N$ , stochastic availability  $\mathcal{B}_t \subseteq [N]$ , and rewards that are sub-Gaussian with parameter  $R^2 = \sigma^2 + L_f^2$  up to a deterministic slack  $s = L_{f'}\Delta$  per pull. Let UCB select  $j_t = \arg \max_{j \in \mathcal{B}_t} (\bar{y}_j + U_j(n_j))$  where  $U_j(n) = R\sqrt{2 \log(4NT/\delta)/n}$ . Define the best available bin as  $j_t^* = \arg \max_{j \in \mathcal{B}_t} \mu_j$ . On  $\mathcal{E}_4$ , we have:*

$$\sum_{t=T_0+1}^T [\mu_{j_t^*} - \mu_{j_t}] \leq 4R\sqrt{NT \log\left(\frac{4NT}{\delta}\right)} + 2sT$$

*Proof.* Note that  $s = L_{f'}\Delta$  represents an irreducible deterministic approximation bias from the within-bin Lipschitz variation. The UCB confidence radius  $U_j(n)$  strictly bounds the stochastic noise and does not inherently absorb this deterministic bias. Instead, the bias propagates additively into the confidence event  $\mathcal{E}_4$ .

On  $\mathcal{E}_4$ , the modified UCB intervals are simultaneously valid:  $|\bar{y}_j - \mu_j| \leq U_j(n_j) + s$ . Fix round  $t$ . Since  $j_t^* \in \mathcal{B}_t$ , the UCB index of the optimal bin satisfies  $\bar{y}_{j_t^*} + U_{j_t^*}(n_{j_t^*}) \geq \mu_{j_t^*} - s$ . By the UCB selection rule,  $\bar{y}_{j_t} + U_{j_t}(n_{j_t}) \geq \bar{y}_{j_t^*} + U_{j_t^*}(n_{j_t^*}) \geq \mu_{j_t^*} - s$ . Combining this with the upper confidence bound on  $j_t$  gives:

$$\mu_{j_t^*} - \mu_{j_t} \leq 2U_{j_t}(n_{j_t}) + 2s$$

Summing over  $t$  and bounding the confidence width sum by grouping rounds per arm yields:

$$\sum_{t=T_0+1}^T U_{j_t}(n_{j_t}) = \sum_{j=1}^N \sum_{n=1}^{N_j(T)} R\sqrt{\frac{2 \log(4NT/\delta)}{n}} \leq \sum_{j=1}^N 2R\sqrt{2N_j(T) \log\left(\frac{4NT}{\delta}\right)}$$

Applying Cauchy-Schwarz with  $\sum_j N_j(T) = T - T_0 \leq T$ :

$$\sum_{j=1}^N \sqrt{N_j(T)} \leq \sqrt{N \sum_{j=1}^N N_j(T)} \leq \sqrt{NT}$$

Therefore,  $\sum_t U_{j_t}(n_{j_t}) \leq 2R\sqrt{2NT \log(4NT/\delta)}$ . Adding the deterministic  $2sT$  sum concludes the proof.  $\square$

**Theorem C.1** (Main Regret Bound). *Under the stated assumptions, ZoomSIB-UCB satisfies, with probability at least  $1 - \delta$ :*

$$R_T \leq \mathcal{O}\left(d^2 T^{2/3} \log^2\left(\frac{dT}{\delta}\right)\right) + 4R\sqrt{NT \log\left(\frac{4NT}{\delta}\right)} + 4L_{f'}T^{2/3} = \tilde{\mathcal{O}}(d^2 T^{2/3})$$

*Proof.* Decompose  $R_T = R_T^{(1)} + R_T^{(2)}$ . The Phase 1 contribution is bounded by Lemma C.1. For Phase 2, on the event  $\mathcal{E}$ , the instantaneous regret satisfies the three-term decomposition. Lemma C.2 controls the sum of terms (i) and (iii), yielding  $2L_f T^{2/3}$ . For term (ii), since the bin of the true optimal arm  $b_t^* \in \mathcal{B}_t$ , we have  $\mu_{j_t^*} \geq \mu_{b_t^*}$  by definition. Thus,  $\mu_{b_t^*} - \mu_{b_t} \leq \mu_{j_t^*} - \mu_{j_t}$ , allowing Lemma C.3 to apply directly:

$$\sum_{t > T_0} \text{(ii)} \leq 4R \sqrt{NT \log \left( \frac{4NT}{\delta} \right)} + 2L_f T^{2/3}$$

Substituting the number of bins  $N = \lceil 2W/\Delta \rceil = \mathcal{O}(T^{1/3} \sqrt{\log(T/\delta)})$ , the stochastic regret scales as:

$$4R \sqrt{NT \log \left( \frac{4NT}{\delta} \right)} = \mathcal{O} \left( T^{2/3} \log \left( \frac{T}{\delta} \right) \right)$$

Combining the terms from both phases completes the proof:

$$R_T = \mathcal{O} \left( d^2 T^{2/3} \log^4 \left( \frac{dT}{\delta} \right) \right) + \mathcal{O} \left( T^{2/3} \log \left( \frac{T}{\delta} \right) \right) + \mathcal{O} \left( L_f T^{2/3} \right) = \tilde{\mathcal{O}}(d^2 T^{2/3})$$

□

## D Proof of Theorem 5.1

### D.1 The Hard Instance

**Parameter choices.** Fix the following parameters throughout the proof:

$$N = \lceil T^{1/3} \rceil, \quad K = \lceil 4N \log T \rceil, \quad \varepsilon = \frac{1}{2N}. \quad (15)$$

**Bins and inner halves.** Partition  $[-1, 1]$  into  $N$  disjoint bins  $B_j = [-1 + \frac{2(j-1)}{N}, -1 + \frac{2j}{N})$  of width  $w = 2/N$ , with centres  $c_j = -1 + w(j - \frac{1}{2})$ . Define the inner half-bin:

$$B_j^\circ = \left[ c_j - \frac{w}{4}, c_j + \frac{w}{4} \right] \subset B_j. \quad (16)$$

These inner halves have width  $w/2 = 1/N$  and are strictly pairwise disjoint.

**Bump functions and Hypothesis Class.** For each  $j \in [N]$ , define the continuous, plateaued bump function  $\psi_j : [-1, 1] \rightarrow [0, 1]$ :

$$\psi_j(z) = \begin{cases} 1 & \text{if } z \in B_j^\circ, \\ 1 - \frac{4}{w} (|z - c_j| - \frac{w}{4}) & \text{if } z \in B_j \setminus B_j^\circ, \\ 0 & \text{otherwise.} \end{cases} \quad (17)$$

By construction,  $\psi_j$  equals 1 on  $B_j^\circ$ , vanishes outside  $B_j$ , and satisfies  $\|\psi_j'\|_\infty \leq 4/w = 2N$  almost everywhere. For each  $\beta \in \{-1, +1\}^N$ , define the associated link function:

$$f_\beta(z) = \frac{1}{2} + \varepsilon \sum_{j=1}^N \beta_j \psi_j(z), \quad \forall z \in [-1, 1]. \quad (18)$$

**Lemma D.1** (Validity of the Instance). *For every  $\beta \in \{-1, +1\}^N$ , the function  $f_\beta$  satisfies the core assumptions: (a)  $\|f_\beta\|_\infty \leq \frac{1}{2} + \varepsilon \leq 1 \leq L_f$ ; (b)  $\|f_\beta'\|_\infty = 2\varepsilon N = 1 \leq L_{f'}$  almost everywhere; and (c)  $f_\beta \equiv \frac{1}{2} + \varepsilon \beta_j$  on  $B_j^\circ$ .*

*Remark:* A standard mollification  $\tilde{f}_\beta = f_\beta * \rho_\eta$  with bandwidth  $\eta = T^{-10}$  ensures infinite differentiability while preserving the uniform bounds and changing the expected regret by merely  $\mathcal{O}(\eta) = o(T^{-9})$ . We analyze the piecewise-linear  $f_\beta$  directly, as expectations change by  $o(1)$ .

## D.2 The Universal Availability Event

To force the algorithm to face an  $N$ -armed bandit, the random menu of arms must cover every inner half-bin. Let  $I_{t,j} = \mathbf{1}_{\{\exists a \in [K]: x_{t,a} \in B_j^\circ\}}$  represent the indicator that an arm lands in the inner half of bin  $j$  at round  $t$ . Define the universal availability event:

$$\mathcal{E} = \{I_{t,j} = 1 \text{ for all } (t, j) \in [T] \times [N]\}. \quad (19)$$

**Lemma D.2** (Availability Probability). *Under  $\mathcal{D} = \text{Unif}[-1, 1]$  and  $K = \lceil 4N \log T \rceil$ , we have  $\mathbb{P}(\mathcal{E}^c) \leq 2T^{-2/3}$ .*

*Proof.* Because  $\mathcal{D}$  has a constant density of  $\frac{1}{2}$  on  $[-1, 1]$ , and  $|B_j^\circ| = w/2 = 1/N$ , the probability that a single drawn context falls into  $B_j^\circ$  is precisely  $\frac{1}{2N}$ . Therefore, the probability that a bin is empty at round  $t$  is:

$$\mathbb{P}(I_{t,j} = 0) = \left(1 - \frac{1}{2N}\right)^K \leq \exp\left(-\frac{K}{2N}\right) \leq \exp(-2 \log T) = T^{-2}.$$

Applying a union bound over  $T \times N$  pairs gives  $\mathbb{P}(\mathcal{E}^c) \leq TN \cdot T^{-2} = N/T$ . Since  $N = \lceil T^{1/3} \rceil \leq 2T^{1/3}$ , we conclude  $\mathbb{P}(\mathcal{E}^c) \leq 2T^{1/3}/T = 2T^{-2/3}$ .  $\square$

*Remark:* The  $2T^{-2/3}$  algebraic decay is perfectly sufficient. The proof later requires the failure probability to satisfy  $2T^{-2/3} \leq 1/(8e)$ , which is strictly met for all  $T \geq (16e)^{3/2} \approx 3600$ .

**Lemma D.3** (Per-Round Regret). *Let  $j_t$  denote the bin of the arm chosen at round  $t$ . Under any hypothesis  $\beta \neq -1$ , conditional on  $\mathcal{E}$ , the instantaneous regret satisfies  $r_t(\beta) \geq \varepsilon \cdot \mathbf{1}_{\{\beta_{j_t} = -1\}}$ .*

*Proof.* On  $\mathcal{E}$ , every inner half-bin  $B_j^\circ$  contains at least one arm. Because  $\beta \neq -1$ , there exists an optimal bin  $j^\star$  where  $\beta_{j^\star} = +1$ . By  $\mathcal{E}$ , there exists an arm  $a^\star$  with  $x_{t,a^\star} \in B_{j^\star}^\circ$ , yielding  $f_\beta(x_{t,a^\star}) = \frac{1}{2} + \varepsilon$ . Thus, the maximum available reward is at least  $\frac{1}{2} + \varepsilon$ . If the algorithm selects an arm in a sub-optimal bin where  $\beta_{j_t} = -1$ , the reward is  $f_\beta(x_{t,a_t}) = \frac{1}{2} - \varepsilon \psi_{j_t}(x_{t,a_t}) \leq \frac{1}{2}$ , ensuring a strictly positive regret of at least  $\varepsilon$ .  $\square$

## D.3 KL Computation and the Bretagnolle-Huber Contradiction

**Proposition D.1** (KL Divergence). *For any algorithm  $\pi$ , hypothesis  $\beta \in \{-1, +1\}^N$ , and bin  $j \in [N]$ , let  $\beta^{\oplus j}$  denote  $\beta$  with the  $j$ -th component flipped. Let  $P_\beta^\pi$  denote the probability measure over the algorithm's history, and  $N_j^\pi(\beta)$  denote the expected number of pulls from bin  $j$ . Then:*

$$\text{KL}\left(P_\beta^\pi \parallel P_{\beta^{\oplus j}}^\pi\right) \leq 2\varepsilon^2 N_j^\pi(\beta). \quad (20)$$

*Proof.* By the chain rule for KL divergence, and because the contexts are drawn independently of  $\beta$ , the divergence accumulates solely from the reward distributions of the selected arms. Because  $f_\beta$  and  $f_{\beta^{\oplus j}}$  differ only inside  $B_j$ , the difference in their means is strictly  $2\varepsilon\beta_j\psi_j(x)$ , which is non-zero only when the chosen arm falls in bin  $j$ . Summing the Gaussian KL divergences  $\frac{1}{2}(\Delta\mu)^2$  over the  $T$  rounds yields the stated bound.  $\square$

*Proof of Theorem 5.1.* Let  $\beta^{(0)} = -\mathbf{1}$  be the *null* hypothesis, and  $\beta^{(j)} = -\mathbf{1} + 2e_j$  be the *spike* hypothesis where bin  $j$  is uniquely optimal. Define the event  $A_j = \{\#\{t : j_t = j\} \geq T/2\}$ .

Under  $\beta^{(j)}$ , on the event  $\mathcal{E} \cap A_j^c$ , the algorithm plays sub-optimal bins ( $\beta_{j_t}^{(j)} = -1$ ) for more than  $T/2$  rounds. By Lemma D.3, the expected regret satisfies:

$$\mathbb{E}_{\beta^{(j)}}[R_T] \geq \frac{\varepsilon T}{2} \mathbb{P}_{\beta^{(j)}}(\mathcal{E} \cap A_j^c) \geq \frac{\varepsilon T}{2} \left(\mathbb{P}_{\beta^{(j)}}(A_j^c) - 2T^{-2/3}\right). \quad (21)$$

To relate the probability measures, we compute the KL divergence under  $\beta^{(0)}$  to control the Bretagnolle-Huber inequality, while the regret is evaluated under  $\beta^{(j)}$ . By Proposition D.1,  $\text{KL}(P_{\beta^{(0)}} \parallel P_{\beta^{(j)}}) \leq 2\varepsilon^2 N_j^\pi(\beta^{(0)})$ . Since

$\sum_j N_j^\pi(\beta^{(0)}) \leq T$ , Markov’s inequality ensures there exists a subset of bins  $J^\star \subseteq [N]$  with  $|J^\star| \geq N/2$  such that for all  $j \in J^\star$ ,  $N_j^\pi(\beta^{(0)}) \leq 2T/N$ . For any  $j \in J^\star$ :

$$\text{KL} \left( P_{\beta^{(0)}} \parallel P_{\beta^{(j)}} \right) \leq 2\epsilon^2 \left( \frac{2T}{N} \right) = \frac{T}{N^3} \leq 1,$$

where we substituted  $\epsilon = 1/(2N)$  and  $N = \lceil T^{1/3} \rceil$ .

The Bretagnolle-Huber inequality dictates that:

$$\mathbb{P}_{\beta^{(0)}}(A_j) + \mathbb{P}_{\beta^{(j)}}(A_j^c) \geq \frac{1}{2} \exp \left( -\text{KL} \left( P_{\beta^{(0)}} \parallel P_{\beta^{(j)}} \right) \right) \geq \frac{1}{2e}. \quad (22)$$

We now conduct a case analysis on  $J^\star$ :

- **Case A:** Suppose there exists  $j \in J^\star$  such that  $\mathbb{P}_{\beta^{(j)}}(A_j^c) \geq \frac{1}{4e}$ . Assuming  $T$  is large enough that  $2T^{-2/3} \leq \frac{1}{8e}$ , substituting into (21) yields:

$$\mathbb{E}_{\beta^{(j)}}[R_T] \geq \frac{\epsilon T}{2} \left( \frac{1}{8e} \right) = \frac{T}{32e(2N)} \geq \frac{T^{2/3}}{128e}.$$

- **Case B:** Suppose for all  $j \in J^\star$ ,  $\mathbb{P}_{\beta^{(j)}}(A_j^c) < \frac{1}{4e}$ . By (22), this forces  $\mathbb{P}_{\beta^{(0)}}(A_j) > \frac{1}{4e}$  for all  $j \in J^\star$ . Summing over the subset yields:

$$\frac{N}{8e} \leq \sum_{j \in J^\star} \mathbb{P}_{\beta^{(0)}}(A_j) \leq \mathbb{E}_{\beta^{(0)}}[\#\{j : A_j \text{ holds}\}] \leq 2,$$

where the final inequality holds almost surely because no more than two bins can simultaneously receive  $\geq T/2$  pulls over  $T$  rounds. This implies  $N < 16e$ , which is impossible for  $T \geq (16e)^3$ .

Therefore, setting  $T_0 = \lceil (16e)^3 \rceil$ , for all  $T \geq T_0$ , Case A must hold. Taking the supremum over the hypothesis class concludes the proof with  $c = 1/(128e)$ .  $\square$

## E Detailed Experiments

We present an empirical evaluation of ZoomSIB-UCB against three baselines: GSTOR (a *non-monotone* link function based algorithm), ESTOR (a *monotone*-link function based algorithm) Kang et al. [2025], and Random (uniform arm selection). We evaluate performance across three synthetic link functions to stress-test shape-agnosticism: (1) *Quadratic*  $f(z) = -(z-1)^2 + 1$ ; (2) *Asymmetric*  $f(z) = z \cdot e^{-z^2}$ ; and (3) *Zigzag* (multimodal)  $f(z) = \sin(z) + 0.3z$ . Unless stated otherwise,  $d = 10$ , contexts are standard Gaussian,  $K = 20$ , and results average over 30 independent trials with shaded bands indicating  $\pm 1$  standard deviation.

All experiments were conducted on Google Colab with an NVIDIA T4 GPU (12.67 GB RAM). The total compute required was approximately 15 GPU-hours, with the majority of runtime consumed by the horizon and dimension scaling experiments in Section E.1.

**Adaptive Stopping: no knowledge of  $T_0$  (or  $\mu^*$ ) needed.** Theoretically we need to fix  $T_0 = \tilde{O}(d^2 T^{2/3})$ , which may be very large. To resolve this, we equip ZoomSIB-UCB with an adaptive stopping rule that monitors the empirical drift  $\|\hat{\theta}_0^{(t)} - \hat{\theta}_0^{(t-\Delta t)}\|_1$  every  $\Delta t = 100$  rounds, terminating Phase 1 as soon as the drift falls below  $\epsilon = 0.05$ . A hard cap of  $T_0 \leq 0.4T$  is retained as a safety net for low-signal environments. The resulting Auto-Cap metric exposes a clear hierarchy of signal strength across our test functions, as shown in Table 1: high-signal topologies such as Quadratic and Zigzag trigger termination at as little as 1.8% of  $T$ , while the Asymmetric function—whose geometry yields flat zero-gradient tails—correctly prolongs exploration up to 40% at small horizons, with the cap shrinking as  $T$  grows and more signal accumulates.

## E.1 Scaling Dynamics: Horizon and Dimension

We examine scaling dynamics across time horizons  $T \in \{2000, 5000, 10000, 25000, 40000\}$  (fixed  $d = 10$ ) and ambient dimensions  $d \in \{5, 10, 15, 20, 30\}$  (fixed  $T = 40000$ ). As shown in Figure 3 and Table 1, ZoomSIB-UCB achieves strictly sublinear regret and dominates both baselines at every horizon across all functions. The advantage is starkest on the Quadratic and Zigzag geometries, where GSTOR incurs roughly  $7\times$  and  $10\times$  higher regret, respectively, at  $T = 40000$ .

Transitioning to dimension scaling (detailed in Figure 4 and Table 2), because ZoomSIB-UCB operates entirely in the one-dimensional projected index space after the Stein estimation phase, it successfully bypasses the curse of dimensionality that handicaps kernel-based methods: on the Zigzag function, a  $6\times$  increase in dimension ( $d = 5$  to  $d = 30$ ) inflates ZoomSIB’s regret by only  $2.3\times$  (from  $\approx 1530$  to  $\approx 3475$ ), while GSTOR’s regret nearly doubles on an already much higher baseline.

## E.2 Theoretical Verification

To empirically verify our asymptotic guarantees, we investigate the regret growth rate on the Quadratic, Asymmetric, and Zigzag functions at  $d = 10$  for  $T \in \{2000, 5000, 10000, 25000, 40000\}$ . By fitting a log-log linear regression  $\log R_T = \alpha \log T + \text{const}$ , we extract the empirical scaling exponent  $\alpha$ .

Figure 6, 5, and 7 displays the log-log plots with empirical fits against theoretical reference lines for the asymmetric, quadratic and zigzag functions respectively. The empirical slopes for ZoomSIB-UCB remain securely beneath the theoretical worst-case ceiling of  $2/3$  ( $\approx 0.667$ ). This performance gap is anticipated: the  $\Omega(T^{2/3})$  hard instance from Theorem 5.1 relies on highly localized adversarial perturbations. On standard smooth functions, the adaptive rule terminates Phase 1 early, reducing the effective exploration penalty. In contrast, GSTOR adheres strictly to an empirical slope near 0.75, perfectly matching its  $T^{3/4}$  bound Kang et al. [2025], and the Random policy scales linearly at 1.00.

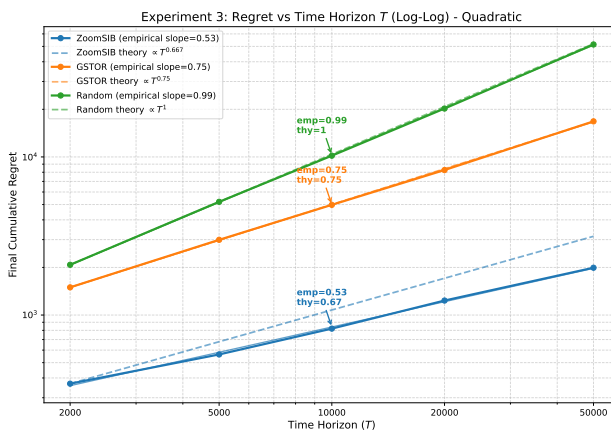
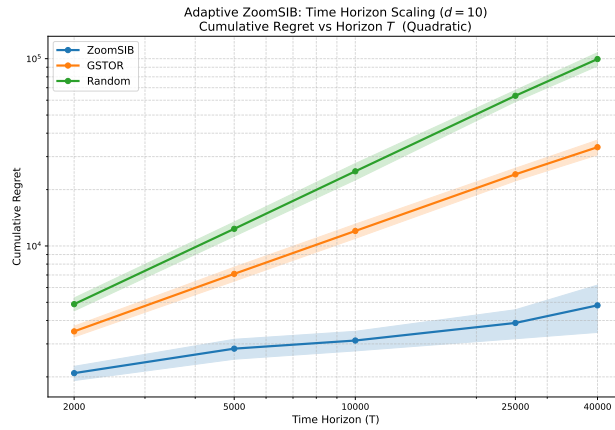
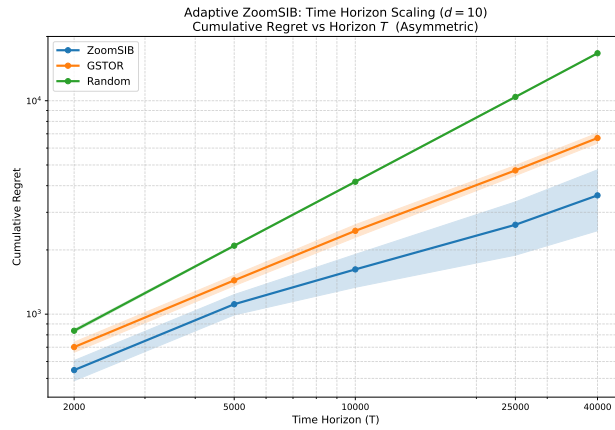


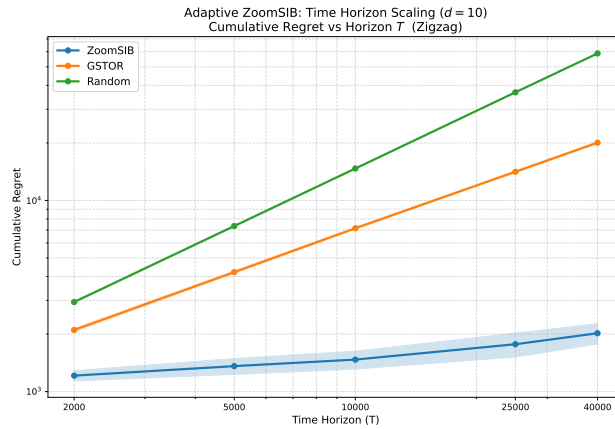
Figure 5: **Log-Log Regret Scaling (Quadratic)**. Empirical (solid) and theoretical reference (dashed) slopes. ZoomSIB achieves an exponent strictly  $< 2/3$ , confirming its sublinear scaling.



(a) Quadratic

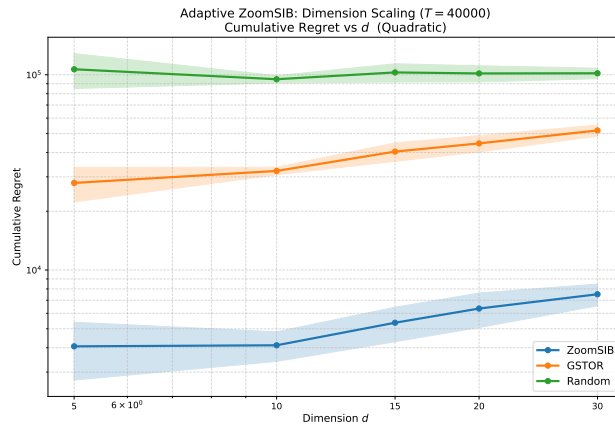


(b) Asymmetric

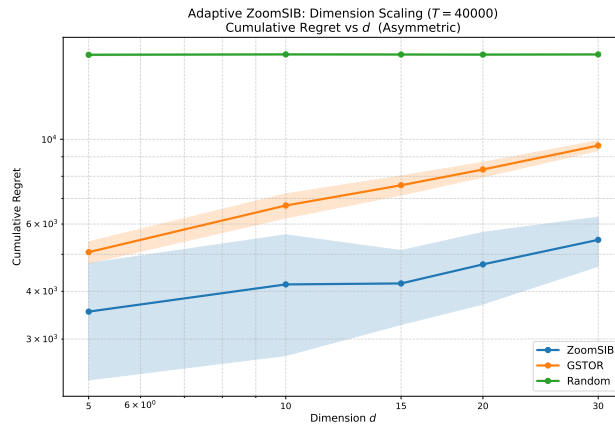


(c) Zigzag

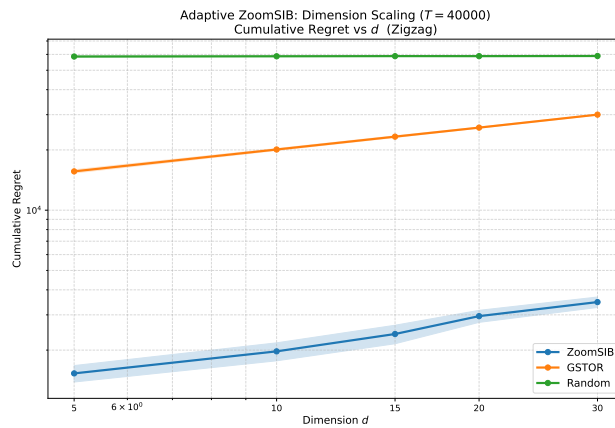
Figure 3: **Horizon Scaling.** Cumulative regret vs. time horizon  $T$  ( $d = 10$ ). ZoomSIB-UCB achieves strictly sublinear regret, significantly outperforming GSTOR and Random exploration across all geometries.



(a) Quadratic



(b) Asymmetric



(c) Zigzag

Figure 4: **Dimension Scaling.** Cumulative regret vs. ambient dimension  $d$  at  $T = 40\,000$ . ZoomSIB-UCB operates entirely in the 1D projected space after Phase 1, successfully avoiding the curse of dimensionality.

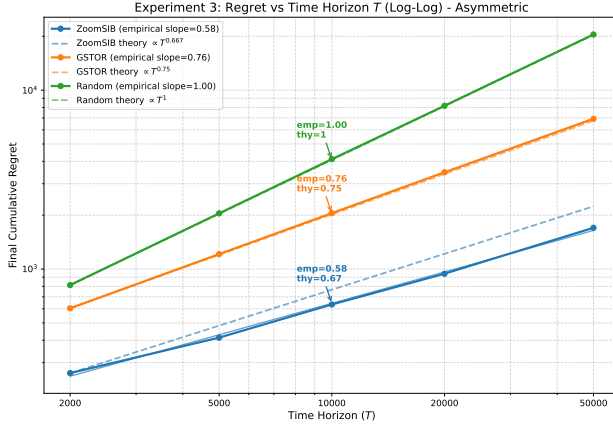


Figure 6: **Log-Log Regret Scaling (Asymmetric)**. Empirical (solid) and theoretical reference (dashed) slopes. ZoomSIB correctly scales sublinearly even with flat, zero-gradient tails.

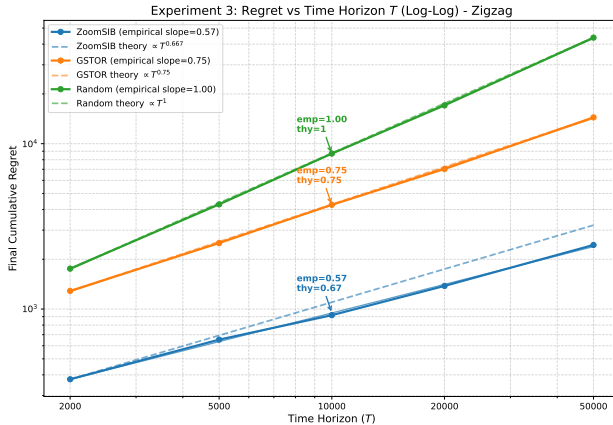


Figure 7: **Log-Log Regret Scaling (Zigzag)**. Empirical (solid) and theoretical reference (dashed) slopes. ZoomSIB easily bypasses the local deceptive optima.

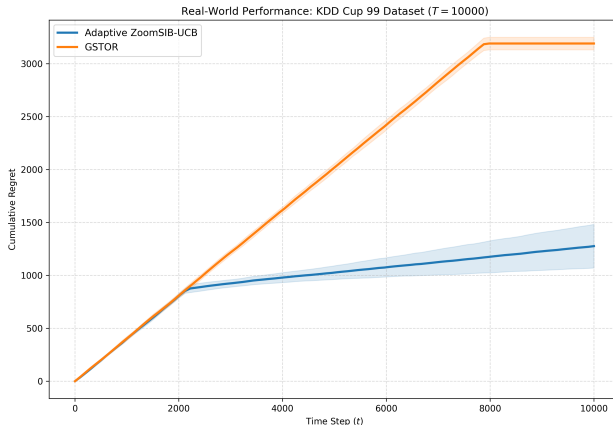
### E.3 Real-World Datasets

We further validate ZoomSIB-UCB on two standard real-world benchmarks: the KDD Cup 99 dataset (Network Intrusion) and the Forest Cover Type dataset. To convert these offline classification datasets into a sequential multi-armed bandit environment, we extract continuous numerical features ( $d = 39$  for KDD 99,  $d = 55$  for Forest Cover) and apply K-Means clustering to partition the data into  $K = 32$  distinct clusters, which serve as our arms. At each round  $t$ , a single observation is randomly sampled from each cluster, and the algorithm must select one. The reward is binary: 1 if the observation belongs to the target class ('normal' traffic for KDD, 'Spruce/Fir' for Forest Cover), and 0 otherwise. Results are averaged over 10 independent runs for  $T = 10\,000$ .

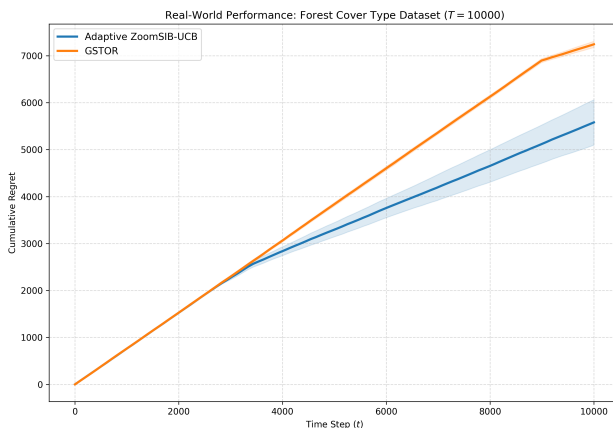
The results expose a severe vulnerability in theoretical exploration bounds when applied to high-dimensional real-world data. Because GSTOR relies on the theoretical formula  $T_1 = \mathcal{O}(d^{3/8}T^{3/4})$ , its double exploration phase mathematically forces it to blindly explore for 79.0% of the rounds in KDD 99 (avg. 7900 rounds) and a crippling 89.9% of the rounds in Forest Cover (avg. 8988 rounds). As a result, GSTOR incurs massive regret:  $3191.30 \pm 59.16$  (KDD 99) and  $7242.70 \pm 67.32$  (Forest Cover).

Conversely, our Adaptive ZoomSIB-UCB dynamically tracks the Stein score and autonomously realizes it has mapped

the feature space long before the theoretical worst-case bound. It triggers an early exit at just 21.1% (KDD 99) and 29.5% (Forest Cover) of the horizon, seamlessly transitioning to UCB exploitation. This self-calibrating mechanism allows `ZoomSIB-UCB` to crush the baseline, achieving a final regret of  $1276.80 \pm 205.90$  on KDD 99 and  $5579.90 \pm 482.60$  on Forest Cover, demonstrating that adaptive variance-tracking is a strict requirement for deploying single-index bandits in the real world.



(a) KDD Cup 99 ( $d = 39, K = 32$ )



(b) Forest Cover Type ( $d = 55, K = 32$ )

Figure 8: **Real-World Datasets.** Cumulative regret on offline classification datasets transformed into contextual bandit environments ( $T = 10\,000$ ). GSTOR’s theoretical constraints force it to over-explore for up to 89.9% of the horizon. In contrast, Adaptive `ZoomSIB-UCB` autonomously detects signal convergence, exiting exploration early and drastically minimizing regret.

#### E.4 Robustness to Model Misspecification

Finally, we test the algorithms in environments where the reward link is fundamentally misspecified for monotone-assumed models. We evaluate two non-monotone environments:  $f(z) = \sin(2z)$  and  $f(z) = \sin(2z) - 0.5z^2$ . The ESTOR algorithm acts as our misspecified baseline, as it structurally assumes  $f$  is non-decreasing.

As illustrated in Figure 9 and Table 3, ESTOR suffers a catastrophic failure under these geometries, collapsing into linear regret growth. On the highly complex asymmetric function  $f(z) = \sin(2z) - 0.5z^2$ , ESTOR actually accumulates significantly more regret than the pure Random baseline. Conversely, `ZoomSIB`’s shape-agnostic architecture effortlessly maintains sublinear regret throughout, terminating with  $16\,430 \pm 5\,773$  cumulative regret against ESTOR’s

67 667 ± 6 814—a 4.1× reduction despite having access to the exact same data stream. This underscores that ZoomSIB’s non-parametric UCB structure over projected bins is not merely a theoretical construct, but a critical necessity for safe deployment in environments where the reward function shape is unknown.

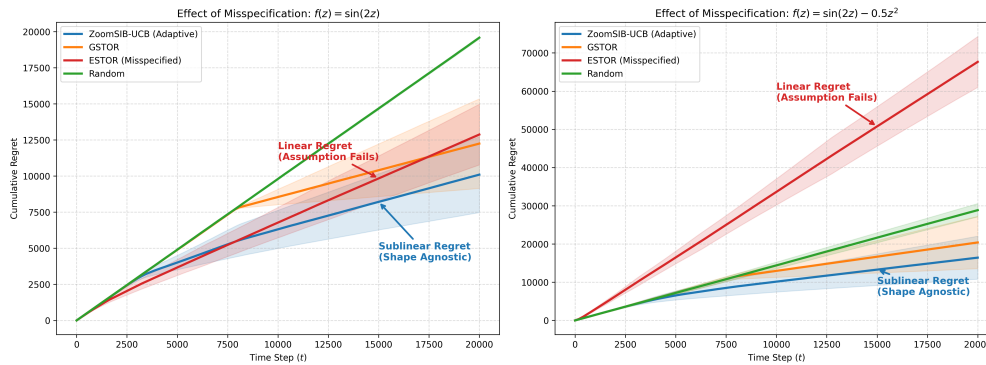


Figure 9: **Model Misspecification.** Cumulative regret vs. time for  $f(z) = \sin(2z)$  (left) and  $f(z) = \sin(2z) - 0.5z^2$  (right). ESTOR (red) collapses to linear regret, while ZoomSIB-UCB (blue) safely maintains sublinear performance.

Table 1: **Horizon Scaling** ( $d = 10$ , mean ± std, 30 trials). ZoomSIB-UCB achieves strictly sublinear cumulative regret across all time horizons and all three link functions, consistently outperforming both GSTOR and Random.

Function	$T$	Auto-Cap	ZoomSIB	GSTOR	Random
Quadratic	2 000	37.5% (750)	<b>2094.04 ± 182.92</b>	3498.31 ± 232.55	4889.82 ± 386.31
	5 000	16.7% (835)	<b>2829.68 ± 345.38</b>	7096.14 ± 609.67	12344.40 ± 1079.93
	10 000	9.1% (910)	<b>3127.09 ± 375.01</b>	12024.97 ± 1049.10	25038.09 ± 2517.72
	25 000	3.4% (860)	<b>3880.88 ± 684.64</b>	24130.01 ± 1871.97	63383.17 ± 4402.28
	40 000	2.2% (865)	<b>4817.61 ± 1363.25</b>	33681.45 ± 3062.29	99524.59 ± 8138.95
Asymmetric <sup>†</sup>	2 000	40.0% (800)	<b>546.98 ± 59.40</b>	701.19 ± 38.31	836.28 ± 13.61
	5 000	34.7% (1735)	<b>1113.31 ± 121.85</b>	1440.38 ± 81.77	2092.67 ± 16.69
	10 000	18.0% (1800)	<b>1620.83 ± 284.94</b>	2457.03 ± 167.55	4173.12 ± 29.91
	25 000	7.2% (1790)	<b>2623.32 ± 734.01</b>	4716.67 ± 257.20	10417.17 ± 48.78
	40 000	4.6% (1825)	<b>3602.55 ± 1143.70</b>	6685.82 ± 363.28	16688.73 ± 73.85
Zigzag	2 000	38.0% (760)	<b>1212.16 ± 74.78</b>	2100.81 ± 47.02	2941.98 ± 27.75
	5 000	14.8% (740)	<b>1359.30 ± 128.93</b>	4216.63 ± 73.79	7347.30 ± 76.38
	10 000	7.7% (770)	<b>1470.57 ± 158.39</b>	7154.54 ± 94.58	14691.33 ± 121.01
	25 000	3.0% (745)	<b>1769.33 ± 252.53</b>	14125.67 ± 177.18	36794.13 ± 207.85
	40 000	1.8% (730)	<b>2020.43 ± 246.92</b>	20055.38 ± 261.18	58775.07 ± 283.15

<sup>†</sup>Note on Auto-Cap: The Asymmetric function requires a substantially longer Phase 1 exploration at smaller horizons because its geometry features flat, zero-gradient tails, yielding a weaker initial signal. The adaptive rule autonomously detects this and correctly prolongs exploration until the Stein estimator safely converges.

Table 2: **Dimension Scaling** at  $T = 40\,000$  (mean  $\pm$  std, 30 trials). Random omitted.

Function	$d$	Auto-Cap	ZoomSIB	GSTOR
Quadratic	5	1.7% (695)	<b>4065.17 <math>\pm</math> 1335.59</b>	27924.93 $\pm$ 5616.88
	10	2.1% (825)	<b>4115.63 <math>\pm</math> 711.70</b>	32166.26 $\pm$ 1420.25
	15	2.9% (1140)	<b>5369.42 <math>\pm</math> 1076.47</b>	40399.23 $\pm$ 4371.87
	20	3.0% (1220)	<b>6348.24 <math>\pm</math> 1274.46</b>	44514.44 $\pm$ 4258.43
	30	4.3% (1710)	<b>7512.44 <math>\pm</math> 959.54</b>	51858.21 $\pm$ 3380.79
Asymmetric	5	2.5% (1015)	<b>3539.72 <math>\pm</math> 1194.59</b>	5065.32 $\pm$ 327.35
	10	4.3% (1720)	<b>4170.52 <math>\pm</math> 1453.64</b>	6709.79 $\pm$ 488.31
	15	5.9% (2350)	<b>4194.86 <math>\pm</math> 920.30</b>	7580.89 $\pm$ 440.49
	20	7.4% (2980)	<b>4705.24 <math>\pm</math> 1000.94</b>	8334.85 $\pm$ 371.19
	30	8.8% (3515)	<b>5455.79 <math>\pm</math> 801.33</b>	9629.01 $\pm$ 287.24
Zigzag	5	1.6% (630)	<b>1530.02 <math>\pm</math> 144.51</b>	15625.01 $\pm$ 291.38
	10	1.9% (765)	<b>1971.39 <math>\pm</math> 203.27</b>	20096.80 $\pm$ 226.58
	15	2.5% (985)	<b>2407.08 <math>\pm</math> 255.51</b>	23296.45 $\pm$ 226.13
	20	2.9% (1175)	<b>2956.26 <math>\pm</math> 204.58</b>	25848.30 $\pm$ 162.75
	30	4.0% (1610)	<b>3475.11 <math>\pm</math> 208.71</b>	30011.30 $\pm$ 170.86

Table 3: **Final cumulative regret** at  $T = 20\,000$  (mean  $\pm$  std, 30 trials).

Function	Auto-Cap	ZoomSIB	GSTOR	ESTOR (misspec.)	Random
$f(z) = \sin(2z)$	15.0% (3005)	<b>10097 <math>\pm</math> 2691</b>	12246 $\pm$ 3181	12874 $\pm$ 2154	19580 $\pm$ 87
$f(z) = \sin(2z) - 0.5z^2$	20.1% (4010)	<b>16430 <math>\pm</math> 5773</b>	20406 $\pm$ 7027	67667 $\pm$ 6814	28857 $\pm$ 1779